Brain, Behavior, & Immunity - Health 26 (2022) 100556

Contents lists available at ScienceDirect

Brain, Behavior, & Immunity - Health

journal homepage: www.editorialmanager.com/bbih/default.aspx

Exercise facilitates regeneration after severe nerve transection and further modulates neural plasticity

Yunfan Kong [a,b], Mitchell Kuss [a,b], Yu Shi [c], Fang Fang [a,b], Wen Xue [a,b], Wen Shi [a,b], Yutong Liu [d], Chi Zhang [c,e], Peng Zhong [f], Bin Duan [a,b,g,h,*]

[a] Mary & Dick Holland Regenerative Medicine Program, University of Nebraska Medical Center, Omaha, NE, 68198, USA
[b] Division of Cardiology, Department of Internal Medicine, University of Nebraska Medical Center, Omaha, NE, 68198, USA
[c] School of Biological Sciences, University of Nebraska Lincoln, Lincoln, NE, 68588, USA
[d] Department of Radiology, University of Nebraska Medical Center, Omaha, NE, 68198, USA
[e] Center for Plant Science Innovation, University of Nebraska-Lincoln, Lincoln, NE, 68588, USA
[f] Department of Neurological Sciences, University of Nebraska Medical Center, Omaha, NE, 68198, USA
[g] Department of Surgery, College of Medicine, University of Nebraska Medical Center, Omaha, NE, 68198, USA
[h] Department of Mechanical and Materials Engineering, University of Nebraska-Lincoln, Lincoln, NE, 68588, USA

ARTICLE INFO

Keywords:
Long-gap nerve transection
Treadmill exercise
Rehabilitation
Nerve regeneration
Neuroplasticity
MEMRI

ABSTRACT

Patients with severe traumatic peripheral nerve injury (PNI) always suffer from incomplete recovery and poor functional outcome. Physical exercise-based rehabilitation, as a non-invasive interventional strategy, has been widely acknowledged to improve PNI recovery by promoting nerve regeneration and relieving pain. However, effects of exercise on chronic plastic changes following severe traumatic PNIs have been limitedly discussed. In this study, we created a long-gap sciatic nerve transection followed by autograft bridging in rats and tested the therapeutic functions of treadmill running with low intensity and late initiation. We demonstrated that treadmill running effectively facilitated nerve regeneration and prevented muscle atrophy and thus improved sensorimotor functions and walking performance. Furthermore, exercise could reduce inflammation at the injured nerve as well as prevent the overexpression of TRPV1, a pain sensor, in primary afferent sensory neurons. In the central nervous system, we found that PNI induced transcriptive changes at the ipsilateral lumber spinal dorsal horn, and exercise could reverse the differential expression for genes involved in the Notch signaling pathway. In addition, through neural imaging techniques, we found volumetric, microstructural, metabolite, and neuronal activity changes in supraspinal regions of interest (i.e., somatosensory cortex, motor cortex, hippocampus, etc.) after the PNI, some of which could be reversed through treadmill running. In summary, treadmill running with late initiation could promote recovery from long-gap nerve transection, and while it could reverse maladaptive plasticity after the PNI, exercise may also ameliorate comorbidities, such as chronic pain, mental depression, and anxiety in the long term.

1. Introduction

Peripheral nerve injury (PNI) is a common cause of traumatic injury, affecting over one million people worldwide annually (Daly et al., 2012; Siemionow and Brzezicki, 2009). Traumatic PNIs usually occur in the upper limbs, which could be the results from a variety of causes, including stabbing, direct trauma, motor vehicle accident, and so on, and often result in sensorimotor function deficits, weakness, and persistent neuropathic pain (Lizeth Castillo-Galvan et al., 2014). Although peripheral nerves have the intrinsic capability of spontaneous regeneration to some degree, the process is slow and often has poor functional outcomes (Höke, 2006). Therefore, patients with severe neurotmesis always suffer from an impaired quality of life and profound psychosocial burdens for months or even years.

Regular exercise has been perceived worldwide to promote wellness and quality of life. Growing evidence shows that physical activity and exercise interventions, as a behavioral and non-pharmacological method, can offer benefits in PNI recovery (Maugeri et al., 2021). After a PNI, chronic denervation in targeted muscles will cause a deprivation of trophic factors, myofiber atrophy, and apoptosis of

* Corresponding author. Mary & Dick Holland Regenerative Medicine Program, University of Nebraska Medical Center, Omaha, NE, 68198, USA.
E-mail address: bin.duan@unmc.edu (B. Duan).

https://doi.org/10.1016/j.bbih.2022.100556
Received 15 September 2022; Received in revised form 3 November 2022; Accepted 11 November 2022
Available online 12 November 2022

muscular satellite cells, which in turn negatively affect nerve regeneration and impair muscle restoration after reinnervation (Gordon et al., 2011; Faroni et al., 2015). Motor rehabilitation approaches have exhibited positive effects for strengthening muscles and regaining motor functions in patients with many neurological conditions (Mang and Peters, 2021). In preclinical rodent models with PNIs, exercise training can promote axonal growth and enhance functional reinnervation (English et al., 2009; Wilhelm et al., 2012; Park and Höke, 2014). Moreover, exercise is also helpful for ameliorating PNI-induced pain responses by reducing peripheral inflammation, glial activation, and inflammation in the spinal cord and for enhancing inhibitory regulation in pain transmission in the spinal cord as well as supraspinal regions (Chen et al., 2012; Bobinski et al., 2011; Almeida et al., 2015; Kami et al., 2017). However, most beneficial effects of exercise training (like treadmill and swimming) have currently been reported in nerve transections with tension-free neurorrhaphy, and only a few studies are related to transected long-gap nerve injuries (Maugeri et al., 2021; Wilhelm et al., 2012; Liao et al., 2017; Seta et al., 2018). In addition, these studies implemented nerve glues or silicon/acellular conduits, which are not standard repair approaches. Therefore, the impact of exercise needs to be further assessed on more severe PNI conditions (i.e., long-gap nerve transection) with more clinically relevant repair (i.e., autograft).

PNIs and concomitant neuropathic pain can both structurally and functionally trigger maladaptive changes in the central nervous system (CNS), further inducing chronic pain and emotional and cognitive problems (Taylor et al., 2009; Seminowicz et al., 2009; Yang and Chang, 2019). Exercise may have the capability of regulating the maladaptive changes in brain after PNIs. For instance, recently, exercise has been reported to regulate the activity of excitatory/inhibitory neurons in the limbic area of the brain that is crucial for the emotional aspect of chronic pain, such as fear, anxiety and depression (Kami et al., 2020). Additionally, it has been reported that treadmill exercise caused an enhancement in serotonergic and noradrenergic modulation of anti-nociception as well as suppression of inflammation in several supraspinal regions, such as brainstem and periaqueductal grey (PAG), after PNI (Bobinski et al., 2015; Lopez-Alvarez et al., 2018). Exercise has also been found to enhance opioid-mediated, pain-inhibitory descending pathways in PAG and rostral ventral the medulla (Kim et al., 2015; Stagg et al., 2011). Overall, these studies suggest that exercise affects a broad range of cortical regions involved in pain ascending, processing, and inhibitory descending pathways. However, the chronic impact of exercise on brain reorganization following PNI is still largely unclear, and it is necessary to specify relevant brain areas during PNI recovery to better assess the benefits of exercise for patients with PNIs.

Herein, we examined the effects of treadmill exercise on functional recovery after a long-gap (10 mm) nerve transection injury in a rat model. PNI recovery was determined based on sensory functions, gait and walking performance, gastrocnemius muscle atrophy, and axonal regeneration (Fig. 1). Neuropathic pain-related changes were determined based on both peripheral and central plasticity, including inflammation, glial cell activation in the spinal cord, and transcriptome analysis in the spinal dorsal horn. Furthermore, we also assessed microstructural brain alterations, metabolite changes, and regional neuronal activity by performing diffusion tensor imaging (DTI), magnetic resonance spectroscopy (MRS), and manganese-enhanced magnetic resonance imaging (MEMRI), respectively.

2. Materials and methods

2.1. Surgical procedure for long-gap sciatic nerve transection and autograft repair

The animal protocol was approved by the IACUC at University of Nebraska Medical Center, and the surgical procedure was described in our previous studies (Wu et al., 2019). Briefly, sixteen adult female Sprague-Dawley rats were randomly assigned to two groups: Sham group (n = 6), and Autograft group (n = 10). After rats were deeply anesthetized by using isoflurane, the sciatic nerve located on the right hindlimb was fully exposed. In the Autograft group, a10 mm-long nerve segment ending 5 mm proximal to the bifurcation was transected, following which the excised nerve segment was inverted and orthotopically transplanted by an end-to-end coaptation. After the subcutaneous wound and skin incision closure, rats received postoperative care and were kept for 16 weeks in standard conditions.

2.2. Experimental design and treadmill running

The overall experimental design is depicted in Fig. 1. Sensory tests were conducted for all rats every week post-injury. At week 10 post-injury, 5 rats were blindly and randomly selected from the Autograft group for treadmill treatment, becoming the Exercise group. Low-intensity treadmill exercise started at a slow speed of 2 m/min, followed by an incremental increase of 2 m/min every 2 min. The treadmill running was conducted at a maximum speed of 8 m/min for 15 min, 5 days a week for 6 weeks. At the end of experiment, rats from each group were anesthetized for a brain imaging study. After animal euthanasia, the ipsilateral gastrocnemius muscle, sciatic nerve, L4/L5 dorsal root ganglia (DRGs), spinal dorsal horn (SDH) on the injury side, as well as the spinal cord, were harvested for further physiological, histological, and biomolecular analysis.

2.3. Mechanical withdrawal thresholds by Von Frey test

The sensory function in response to a mechanical stimulus was evaluated by using an ascending Von Frey test, as described in our previous studies with minor modifications (Kong et al., 2021). Briefly, the rats were placed in plastic chambers on a metal mesh platform (Ugo Basile) and allowed to acclimatize for 30 min before the test. The

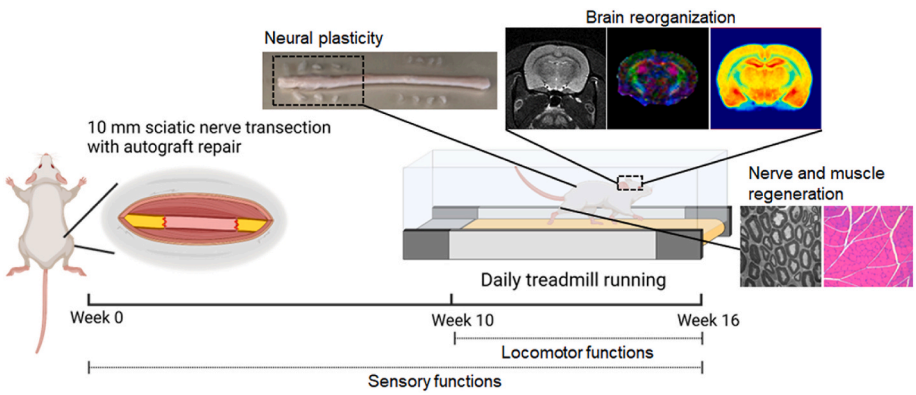

Fig. 1. Schematic of the long-gap sciatic nerve transection, autograft repair, treadmill running paradigm, and experimental design.

mechanical sensory function was tested by applying a series of von Frey filaments (North Coast Medical) to the plantar surface of the hind paw that was operated on. Forces were applied in an ascending order (1, 2, 4, 6, 8, 10, 15, 20 and 50 g) and with a 10 s interval between two stimulations until a withdrawal response (including a stimulus-related lifting or licking) was observed. The ascending procedure was repeated 5 times for each animal, with a 15 min interval between two trials, and the mean was considered as the paw withdrawal threshold. If all filaments failed to induce the response, a cutoff threshold of 50 g was recorded.

2.4. Thermal withdrawal thresholds by Hargreaves test

The thermal sensitivity test was conducted by using a Hargreaves apparatus (Ugo Basile Thermal Plantar Test Instrument). Rats were placed in chambers on a glass panel for 30 min to habituate to the testing environment. An infrared generator was positioned under the panel and applied to the plantar surface of right (operated) hind paw with an infrared intensity of 50. The withdrawal latency was measured automatically by the sensor, and a cutoff time of 30 s was set in each measurement to avoid tissue damage. The test was repeated for 3 times for each animal with a 15 min interval between two stimulations, and the mean was considered as the paw withdrawal latency.

2.5. Walking track analysis

A homemade rat-walking apparatus based on a prototype of a MouseWalker system was used (Mendes et al., 2015). The apparatus was composed of a red backlight top panel, acrylic glass surrounded by green lights, a walking corridor above the glass, and a mirror below the glass that was angled at 45°. Each rat received training to walk from the entrance to the exit of the walking corridor before the test until no distracted or hesitating behaviors were observed during the walking. During the test, rat walking was observed through the mirror and recorded by using a GoPro camera. Gait and movement kinematics were analyzed by using "MouseWalker" software. Results were further calculated and presented as the ratio of the right hind paw to the left hind paw.

2.6. MRS and MRI analysis

MRI/S was performed on a 7 T MRI scanner (Bruker BioSpec 70/21, Billerica) with a Bruker-made quadrature volume coil for signal transmission and receiving. Rats were anesthetized by inhalation of isoflurane in 100% oxygen and maintained 40–80 breaths/minute. Respiration and body temperature were monitored during scanning. ^{1}H MRS data sets were obtained using single voxel semi-LASER (Wijnen et al., 2010) localization with timing parameters (TE/TR = 40/4000 ms, 576 averages, 2048 points). All first and second-order shim terms were first automatically adjusted using MAPSHIM® in ParaVision 6, with a final shim, when necessary, performed manually to achieve a water line width of 10–15 Hz. The water signal was suppressed by variable power RF pulses with optimized relaxation delays (VAPOR) (Tkáč et al., 1999). All MRS data was processed and quantified using LCModel (LCMODEL Inc.). The results were expressed as a percentage of the sum of all 14 metabolites (alanine, aspartic acid, creatine, gamma-aminobutyric acid (GABA), glutamine (Gln), glucose, glutamate (Glu), glycine, glycerophosphocholine, lactic acid, myoinostitiol (Ins), N-acetylaspartate (NAA), phosphocholine, and taurine) as a semi-quantitative method for reporting metabolite concentrations in institutional units (I.U.). Glycerophosphocholine and phosphocholine were added and reported as total choline (tCHO) containing compounds.

DTI was performed using a 4-segment echo planner imaging readout with a balanced, rotationally invariant and alternating polarity icosahedral scheme (12 directions), as detailed in our previous work (Boska et al., 2014), and a b-value = 800 s/mm^2. Maps of the DTI metrics of the apparent diffusion coefficient (ADC) and fractional anisotropy (FA) were calculated using Diffusion Toolkit (Wang and Wedeen. 'http://trackvis.org/dtk/').

For MEMRI, $MnCl_2{\cdot}4H_2O$ (Sigma-Aldrich) was added to 0.9% w/v NaCl (Hospira) to make 50 mM $MnCl_2$ solution. $MnCl_2$ solution was administrated i.p. with a dose of 60 mg/kg four times at 24 h intervals before MRI. After the injections, the rats were observed daily to detect any side effects of $MnCl_2$. MRI data was acquired 24 h after the last $MnCl_2$ administration. The rats were scanned using T1-wt MRI (FLASH, TR = 20 ms, flip angle = 20°). The brain volumes in the T1-wt images were extracted using an in-house Matlab program (Uberti et al., 2009) based on the level sets method. The brain images were then registered to the Schwarz rat brain atlas (Schwarz et al., 2006; Bade et al., 2017) using affine transformation first and then nonlinear transformation, similarly to in previous studies (Devonshire et al., 2017). Signals were normalized to the bilateral visual cortex that was not expected to be activated in the current study (Schwarz et al., 2006).

2.7. Toluidine blue staining and transmission electron microscopy (TEM) imaging

After the brain imaging study, the rats were euthanized and nerve segments were collected from 3 rats in each group. Samples were processed with a fixation with glutaraldehyde and 2% paraformaldehyde (PFA) in a 0.1M Sorenson's phosphate buffer (pH 7.2), post-fixation with 1% aqueous solution of osmium tetroxide, dehydration in a graded ethanol series, and embedment in fresh resin as described in our previous studies (Kong et al., 2021). Thick (1 μm) sections were made with a with a Leica UC7 for toluidine blue staining; thin (100 nm) sections were made with a Leica UC6 Ultracut ultramicrotome for TEM imaging. Images for toluidine blue stained sections were acquired by using an optical microscope. TEM sections were observed on a Tecnai G2 Spirit TWIN (Thermo Fisher Scientific) operating at 80 kV. Nine images of each group were randomly captured, and at least 150 nerve fibers were randomly selected for neural morphological analysis. Areas of axons, myelin sheaths, and whole nerve fibers were measured using ImageJ. The area-based G-ratio was further determined as the ratio of the axon area to the fiber area.

2.8. Wet weight and Hematoxylin and Eosin (H&E) analysis of muscle

Gastrocnemius muscles were collected from the rats, and their wet weights were measured. Subsequently, the gastrocnemius muscles were fixed in 4% PFA solution, dehydrated using ethanol, embedded into paraffin, and transected into 10 μm thick sections. The muscle morphology was determined by using H&E staining. Images for H&E stained sections were acquired by using an optical microscope. The average area for single myofibers was measured using ImageJ.

2.9. Immunostaining

The transected segment of the sciated nerves that were operated on, L4/L5 DRGs, and the lumbar segment of spinal cordssegment were fixed in 4% PFA, cryoprotected in 30% sucrose, and embedded in OCT solution for cryosectioning. Fifteen μm thick sections were made by using a cryotome (CM 1850; Leica). For immunohistochemical (IHC) staining, cryosections were treated with 3% hydrogen peroxide in methanol for 10 min, blocked in 3% normal goat serum in PBS/0.1% Tween-20 solution, and incubated with tumour necrosis factor (TNF)-α antibody overnight (Abcam). A biotinylated goat anti-rabbit secondary antibody was added, followed by the standard DAB procedure for TNF-α detection. Sections were imaged by using optical microscopy. The ratio of brown positive area to total selected area was quantified by using ImageJ software. Staining for gastrocnemius muscle sections was performed on a Discovery Ultra advanced staining system (Roche Diagnostics, Ventana Medical Systems, Inc.). Briefly, sections were deparaffinized, underwent antigen retrieval, and were treated with

Discorvery ChromoMap RUO Inhibitor. Subsequently, samples were incubated with anti-laminin (MilliporeSigma) and anti-Pax 7 (DSHB) for 40 min at 37 °C. Signals were detected and visualized through anti-mouse and anti-rabbit secondary antibody HRP detection, incubation with enzyme conjugate biotin-free Discovery anti-HQ horse-radish peroxidase RTU, and fluorescent staining with Discovery CY5 and FITC RUO. Sections were imaged using a Zeiss 880 LSM, and the frequency of $Pax7^{+}$ cells was measured.

For immunofluorescent (IF) staining of cryosectioned samples, sections were permeabilized and blocked with 0.1% Triton X-100 and 5% goat serum in PBS, followed by incubation with primary antibodies overnight at 4 °C. To be specific, nerve segments were stained with Tubulin β-3 (BioLegend) and myelin basic protein (MBP) (Millipore); L4/L5 DRGs were double stained with Tubulin β-3 (Millipore) and transient receptor potential cation channel subfamily V member 1 (TRPV1) (Alomone Labs) or Cleaved Caspase-3 (Cell Signaling Technology); and spinal cords were double stained with Tubulin β-3 (Millipore) and ionized calcium binding adaptor molecule 1 (Iba-1) (Fujifilm Wako) or glial fibrillary acidic protein (GFAP) (Millipore). After incubation with secondary antibodies and DAPI (Invitrogen), the sections were imaged by a Zeiss 880 LSM. The coherence of axonal alignment, TRPV1 fluorescent intensity of DRGs, and percentage of Iba-1 expressing area of SDHs were measured using ImageJ software.

2.10. TUNEL assay

L4/L5 DRG sections, prepared as described above, were subjected to a TUNEL assay (Roche) according to the manufacturer's instructions. Sections treated with DNase I were used as a positive control, and sections without a reactive solution were used as a negative control. The fluorescent signals were visualized by using a Zeiss 880 LSM.

2.11. RNA sequencing (RNA seq) and bioinformatic analysis

The total RNAs were extracted from ipsilateral SDHs at the lumbar segment by using RNeasy mini kits (QIAGEN) according to the manufacturer's instructions. The RNA sequencing analysis was conducted by LC Sciences (Houston, TX, USA). The quality of each sample was manually inspected using FastQC (http://www.bioinformatics.babraham.ac.uk/projects/fastqc). Barcode removal and filtering and trimming of low-quality reads were executed using the command line tools Trimmomatic (Bolger et al., 2014), and each RNA-seq read was trimmed to make sure the average quality score was larger than 30 and had a minimum length of 70bp. Sequences were aligned to rat reference genomes using HiSET2 (Kim et al., 2019), allowing up to two base mismatches per read. Reads mapped to multiple locations were not considered. The numbers of reads in genes were counted by the software tool HTSeq-count (Anders et al., 2015) using corresponding rat gene annotations, and the "union" resolution mode was used. Genes with a read count lower than 10 across the samples were removed before downstream analysis. Differential expression analysis between the treatment and the control groups was conducted using DESeq2 (Love et al., 2014). Differentially expressed genes were mapped to human orthologs to expand the discovery of possible related signaling pathways. The enriched pathways of differentially expressed genes were identified with Gene Ontology annotations and Kyoto Encyclopedia of Genes and Genomes (KEGG) pathways. A cell signaling network was discovered by mapping the genes with the SIGNOR 2.0 database (Licata et al., 2020), using NetworkAnalyst 3.0 (Zhou et al., 2019). The network analysis was based on the mapped subnetworks with the greatest number of nodes.

2.12. Statistical analysis

All quantitative results were expressed as mean ± standard deviation. Statistical analysis was performed using SPSS statistical software. A two-tailed Student's t-test was used to determine the significant differences between means of two groups. One-way ANOVA was used to determine the significant differences among means of three groups, followed by between-group comparisons with Tukey post-hoc tests or Fisher's LSD tests. A p-value of <0.05 was used as the significance criterion.

3. Results

3.1. Exercise improves sensory functions and gate kinematics after long-gap sciatic nerve transection and autograft repair

A long-gap sciatic nerve transection with an autograft repair was generated in a rat model, and daily low-intensity treadmill exercise was performed from week 10 post-injury until week 16. We first investigated the recovery of sensory functions after the PNI. The sensitivity to the sensation of mechanical stimulation was evaluated by using a Von Frey test, in which the withdraw threshold of the right paw in response to touch stimulus was recorded (Fig. 2A). The long-gap nerve injury caused a complete loss of mechanical sensation. During weeks 5 10 post-injury, the denervated hind paw showed significantly reduced withdraw thresholds, followed by a plateaued recovery process. Then the withdraw threshold progressively decreased, approaching the healthy level, whereas the paws in both the Autograft and Exercise groups still had higher withdrawal thresholds to the stimulus compared to the Sham group at week 16 post-injury. The thermal sensation was evaluated by using the Hargreaves test (Fig. 2B). A severe impairment of the thermal sensory function was caused by the nerve injury, after which the rats could progressively reobtain the thermal sensation up to week 7 post-injury. However, consistent with the recovery of mechanical sensation, the thermal sensation could not be completely recovered at the end of this experiment. As for the rats with treadmill exercise, their withdraw latency was not statistically different from that of the Sham group during the term of treadmill running, implicating that exercise may facilitate recovery of thermal sensation.

For locomotor function recovery, as shown in Fig. 2C, much smaller and dimmer footprints were observed on the side that was operated on as the injured rats were walking, compared to those from the contralateral side as well as from the Sham group. Meanwhile, the paw of the injured hindlimb had touchdown positions further away from the body's center line as well as a shorter stance phase and a longer swing phase relative to that of contralateral paw in the Autograft group and compared to the Sham and Exercise groups (Fig. 2D and E). Quantitative gait analysis further confirmed these observations. Nerve transection caused a much lower brightness intensity of the ipsilateral footprints, indicating that injured hindlimbs could not exert sufficient strength to support the body weight during walking (Fig. 2F). Besides, footprints from the injured paw had a larger perpendicular distance from the body center, implicating that an impaired ability to control the injured hindlimb caused by nerve injury, which was improved over time in the rats with exercise (Fig. 2G). In addition, the PNI severely disrupted the stance/swing phase and slowed the swing speed during walking, reflecting gait deficits and potential painful responses (Fig. 2H and I). At the end of the experiment, exercise progressively and significantly reversed these changes and improved walking performance. All these results suggest that treadmill exercise improved the recovery of sensory functions and locomotor kinematics.

3.2. Exercise reduces in situ inflammation and promotes regrowth and remyelination of transected axons

To investigate the effect of treadmill exercise on the nerve after long-gap transection, autograft nerve segments were sectioned for histological analysis. Local inflammation was determined by IHC staining for TNF-α. The nerve injury dramatically induced the expression of TNF-α at 16 weeks post-injury, which was effectively prevented through treadmill

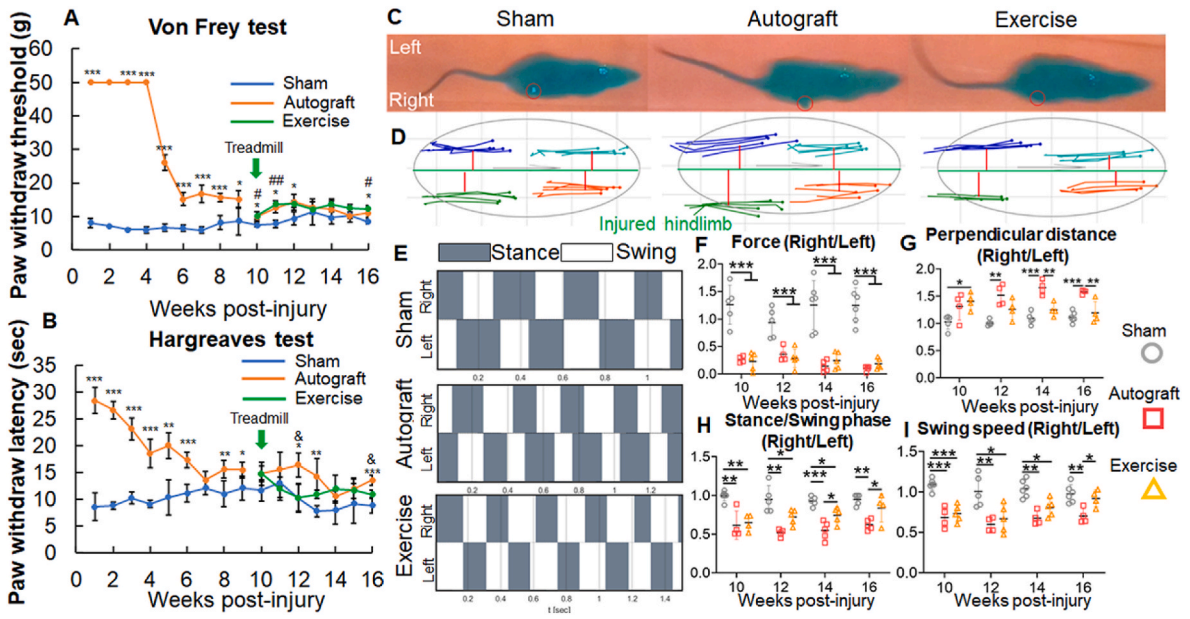

Fig. 2. Mechanical and thermal sensory functions as well as locomotor functions were determined at predetermined time points post-injury. A Withdrawal threshold of the right hind paw in response to mechanical stimuli measured by using a Von Frey test; **B** Latency of the right hind paw in response to heat stimuli measured with a Hargreaves test. (Sham vs Autograft: *p < 0.05, **p < 0.01, ***p < 0.001; Sham vs Exercise: #p < 0.05, ##p < 0.01; Autograft vs Exercise: &p < 0.05, n = 4 or 5); **C** Photographs recorded during rats walking inside a self-built rat-walking apparatus. The red circle indicates a touchdown point of the right hind paw; **D** Representative plots of stance traces of each paw during rat walking. The relative perpendicular distance from each paw to the green central body line was indicated with a red line; **E** Gait patterns indicating swing phases and stance phases for both hind paws; **F–I** Quantitative data analysis for the relative force (**F**), perpendicular distance from paw to the central body line (**G**), stance/swing phase (**H**), and swing speed (**I**) based on the ratio of the right (operated) to left (unoperated) hind paw. (*p < 0.05, **p < 0.01, ***p < 0.001, n = 4 or 5). (For interpretation of the references to color in this figure legend, the reader is referred to the Web version of this article.)

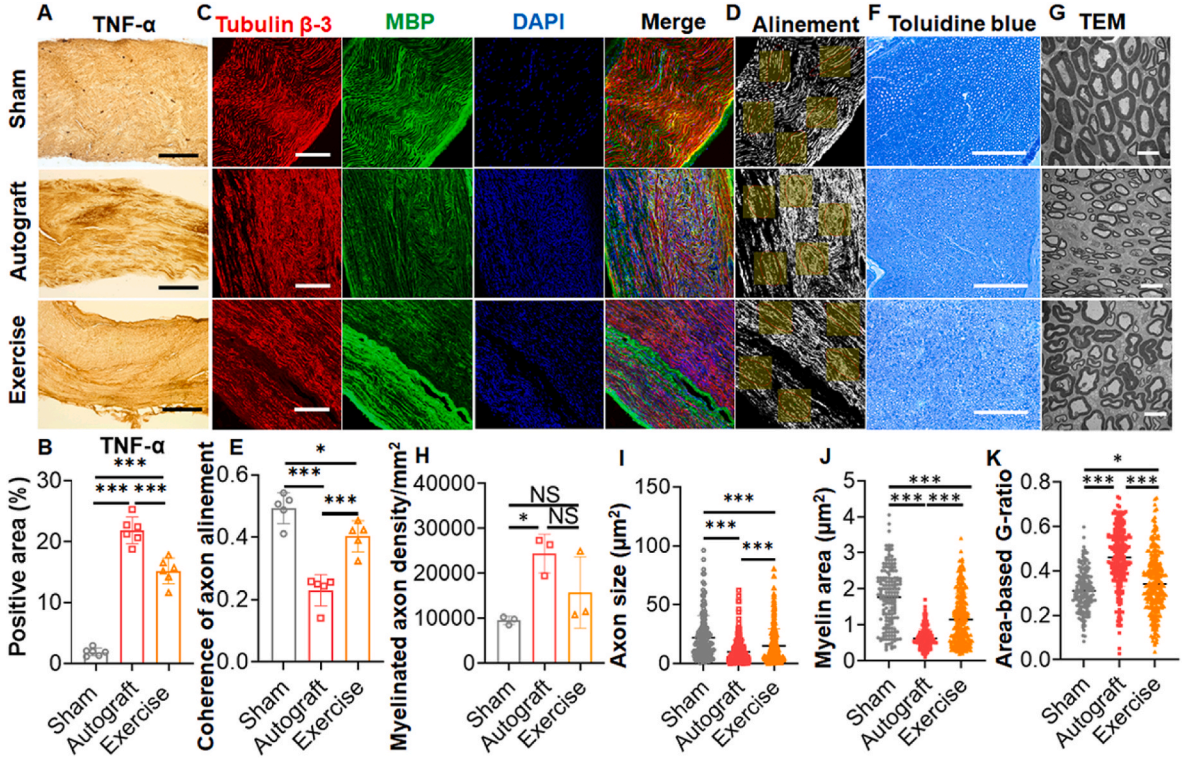

Fig. 3. Histological and morphological analysis of ipsilateral nerve segments. A-B Longitudinal-sectional IHC staining for TNF-α (Scale bar: 200 μm) (**A**) and quantification of the TNF-α positive area (n = 6) (**B**) at right sciatic nerve segments; **C** Longitudinal-sectional IF staining with general nerve marker (Tubulin β-3) and myelin marker (MBP) (Scale bar: 200 μm); **D-E** Measurement of axonal alignment at the right nerve segments, based on IF images (**D**) and quantitative results (n = 5) (**E**); **F-G** Cross-sectional toluidine blue staining (Scale bar: 200 μm) (**F**) and TEM images (Scale bar: 10 μm) (**G**) of the right nerve segments; **H–K** Quantitative data of myelinated axon density (n = 3) (**H**), size of myelinated axons (**I**), myelin area (**J**), and area-based G-ratio (**K**) in single nerve fibers. (*p < 0.05, **p < 0.01, ***p < 0.001). (For interpretation of the references to color in this figure legend, the reader is referred to the Web version of this article.)

exercise (Fig. 3A and B). In addition, IF images of the injured nerve (both Autograft and Exercise groups) showed weaker expression of MBP and increased cell accumulation compared to the Sham group, indicating a severe disruption of myelination and proliferation of SCs (Fig. 3C and Supplementary Fig. 1). Moreover, the nerve injury gave rise to the formation of a nerve coil structure with poor axonal alignment (Fig. 3D and E). This misdirection of axons during regrowth could result in a failure of reinnervation of the target muscle or skin. Treadmill exercise effectively reduced the nerve misdirection and improved the axonal alignment (Fig. 3E).

To further determine the remyelination of the injured nerve, toluidine blue staining and TEM analysis were conducted on cross sections of autograft nerve segments (Fig. 3F and G). The images showed an impaired nerve structure with smaller neural fibers and thinner myelin sheaths after the injury. Compared to the Autograft group, larger neural fibers with thicker myelin sheaths were observed in the Exercise group. Statistical analysis based on TEM images revealed that the myelinated axons appeared after the nerve injury, reflecting an undergoing regenerative process (Fig. 3H). However, consistent with the observation, regenerated neural fibers in the Autograft group were in small size with thin myelin sheaths compared to Sham and Exercise groups (Fig. 3I and J). Treadmill exercise significantly promoted axons to grow larger and be wrapped with thicker myelin sheaths. The G-ratio is an important functional and structural index of axonal myelination, with a smaller G-ratio reflecting higher axonal myelination. The area-based G-ratio was measured in single neural fibers, and the result demonstrated that the nerve injury caused a significant increase in the G-ratio, which was reversed by the treadmill exercise, reflecting an improved remyelination (Fig. 3K). Together with all these results, exercise ameliorated *in situ* inflammation of transected nerve segments and, meanwhile, promoted nerve regeneration and remyelination.

3.3. Exercise prevents gastrocnemius muscle atrophy after long-gap sciatic nerve transection and autograft implantation

At 16 weeks post-injury, ipsilateral gastrocnemius muscles were collected to determine muscle quality. The nerve injury resulted in a significant wet weight loss of gastrocnemius muscles, which was prevented by exercise training to some extent (Fig. 4A and B). Meanwhile, the atrophy of skeletal myofibers was also observed based on the average size of the myofibers, which was ameliorated after exercise (Fig. 4C and D). Thus, exercise could offer beneficial effects to prevent muscle atrophy after denervation. Skeletal muscle stem cells, also referred as satellite cells, can become activated and are critical in myofiber hypertrophy and growth after damage. Thus, the density of Pax 7^{+} satellite cells were calculated to evaluate the regenerative ability of gastrocnemius muscles. As shown in Fig. 4E and F, the PNI slightly decreased the frequency of Pax 7^{+} satellite cells. Compared to the Autograft group, more Pax 7^{+} cells were observed in the rats with exercise, suggesting that exercise may prevent the depletion of the satellite cell pool after long-term denervation and thus helps maintain the regenerative ability.

3.4. Long-gap nerve transection persistently causes increased expression of TRPV1 in the L4/L5 DRGs and microgliosis in the spinal cord

Neuropathic pain after PNI could result from dysfunctional changes in both peripheral and central nervous systems (Meacham et al., 2017). Herein, plastic changes after the long-gap nerve transection were investigated in the L4/L5 DRGs as well as in the spinal cord of the lumbar segment. Based on IF staining, DRG neurons did not show differential expression of cleaved casepase-3, a marker for apoptosis, at 16 weeks post-injury (Supplementary Fig. 2A). Consistently, the TUNNEL assay also turned out no significant apoptosis in the DRGs after the nerve injury (Supplementary Fig. 2B). Meanwhile, DRG neurons highly

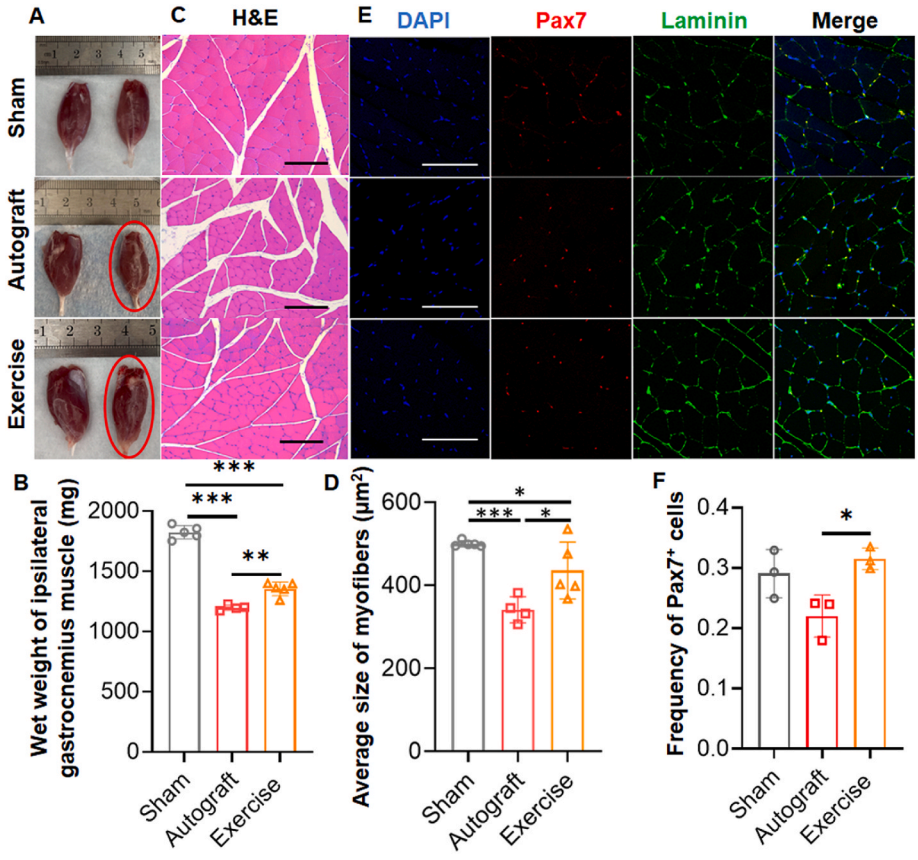

Fig. 4. Muscular wet weight and histological analysis at ipsilateral gastrocnemius muscles. A Representative photographs of gastrocnemius muscles from hindlimbs. Muscles indicated by a red circle were from injured hindlimbs; **B** Wet weight of gastrocnemius muscles from the right side (n = 5); **C** Cross-sectional H&E images of right gastrocnemius muscles (Scale bar: 100 μm); **D** Average size of single myofibers in right gastrocnemius muscles (n = 4 or 5); **E** Cross-sectional IF staining with Pax7 and laminin of right gastrocnemius muscles (Scale bar: 100 μm); **F** Frequency of Pax7^{+} cells in right gastrocnemius muscles (n = 3). (*p < 0.05, **p < 0.01, ***p < 0.001). (For interpretation of the references to color in this figure legend, the reader is referred to the Web version of this article.)

expressed TRPV1 receptor, a molecular integrator of nociceptive stimuli (Fig. 5A). A high expression of TRPV1 receptors in nociceptors is commonly associated with thermal hyperalgesia during neuropathic pain and inflammatory pain. Therefore, DRG sensory neurons could survived the acute damage caused by the nerve transection, but, meanwhile, they also underwent long-term changes that may lead to hypersensitivity and pain. The fluorescent intensity of expressed TRPV1 significantly increased after long-gap nerve transection and autograft repair, although further exercise training decreased the TRPV1 expression when compared with the Autograft group (Fig. 5B). In the lumbar segment of SDHs, a dramatically increased expression of Iba-1, the microglia marker, has been found in both ipsilateral and contralateral sides in both Autograft and Exercise groups after the PNI (Fig. 5C and D, and Supplementary Fig. 2C). Microglial proliferation and activation have been widely reported in neuropathic pain and are considered as crucial reasons for the development and maintenance of PNI-induced pain. Nevertheless, no differential expressions of TNF-α or GFAP, an astrocyte marker, were revealed at 16 weeks after the nerve transection, based on immunohistology analysis (Supplementary Figs. 2D and E). This suggests that there is less initial pain from the acute nerve injury but rather a widespread and vague pain.

3.5. *Long-gap nerve transection causes chronic transcriptome profiling changes in the right SDHs, and exercise partially reverses the differential expression of genes*

To further investigate transcriptome changes in the spinal cord after the nerve transection and the following exercise, the lumbar SDHs ipsilateral to the injury were collected for RNA-Seq analysis. A total of 13,684 RNA transcripts have been identified, and 565 detected differentially expressed genes (DEGs) were displayed in a heat map (Fig. 6A and Supplementary Table 1) and a Venn diagram (Fig. 6B and Supplementary Table 2). When comparing the Autograft group to the Sham group, a total of 220 DEGs were detected, with 198 of them being upregulated and 22 being downregulated (Fig. 6C). DEGs with a p-value < 0.05 and a fold change >2 were selected for the KEGG enrichment analysis. With a p-value < 0.05 for the threshold of significant enrichment, DEGs after the nerve transection were enriched in ErbB signaling, glioma, neurotrophin signaling, PI3K-Akt signaling, and MAPK signaling pathways (Supplementary Fig. 3A). These pathways have critical functions in neural survival, neurogenesis, and long-term potentiation (Skaper, 2018; Ding et al., 2021) as well as glial regulation and inflammation (Chen et al., 2017a; Lin et al., 2014) in the central nervous system. Furthermore, downregulated and upregulated DEGs were analyzed. Downregulated DEGs were enriched in 14 pathways, including pathways associated with the GABAergic synapse, cholinergic synapse, glutamatergic synapse, serotonergic synapse, and dopaminergic synapse (Fig. 6D), reflecting a synaptic remodeling following the nerve injury. Upregulated DEGs were enriched in 33 pathways, and the activation of some pathways, such as the Jak/STAT signaling pathway, neurotrophin signaling pathway, and Notch signaling pathway (Fig. 6E), can promote neural stem cell proliferation and differentiation but also induce inflammation and central sensitization. Furthermore, 75 DEGs were detected by comparing the Exercise group with the Autograft group (Fig. 6F). However, only limited KEGG pathways were identified, which have poor association with nerve lesions (Supplementary Fig. 3B). To better understand the therapeutic effect of exercise during PNI recovery, we selected transcriptive genes that were differentially expressed after the nerve transection and recovered to the healthy level after the treadmill training. A total of 71 DEGs were screened out, and they were enriched in 10 signaling pathways, including Notch signaling and T cell differentiation (Fig. 6G and Supplementary Table 3). In addition, the cell signaling network analysis also identified the *Jag1/-Notch1/Hoxa5* signaling as a central hub of DEGs (Fig. 6H). These results suggest a critical role of the Notch signaling in the spinal cord after traumatic PNI as well as during the exercise-mediated recovery.

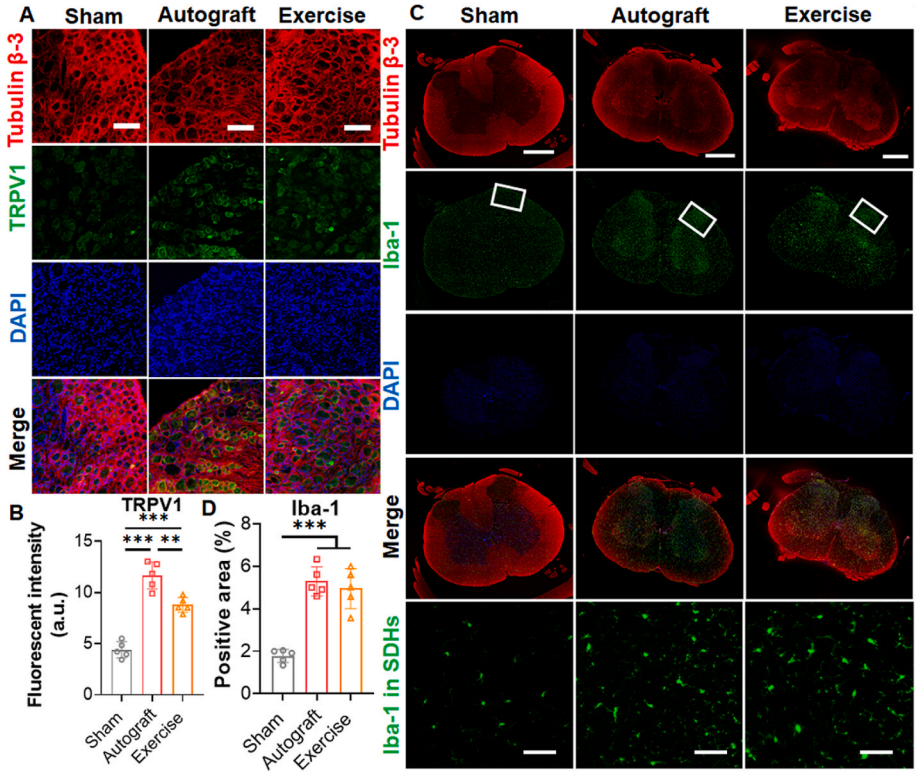

Fig. 5. IF staining for plastic changes in right lumbar L4/L5 DRGs as well as in spinal cords. A Right lumbar L4/L5 DRGs double stained with tubulin β-3 and TRPV1, a pain receptor expressed on sensory neurons (Scale bar: 100 μm); **B** Fluorescent intensity of TRPV1 based on DRG IF images (n = 5); **C** Cross-sectional lumbar spinal cords double stained with tubulin β-3 and Iba-1, a microglial marker (Scale bar: 1000 μm), and Iba-1 expression at right SDHs, as indicated by white rectangular areas (Scale bar: 100 μm); **D** Quantitation of Iba-1 positive area at right SDHs (n = 5). (**p < 0.01, ***p < 0.001).

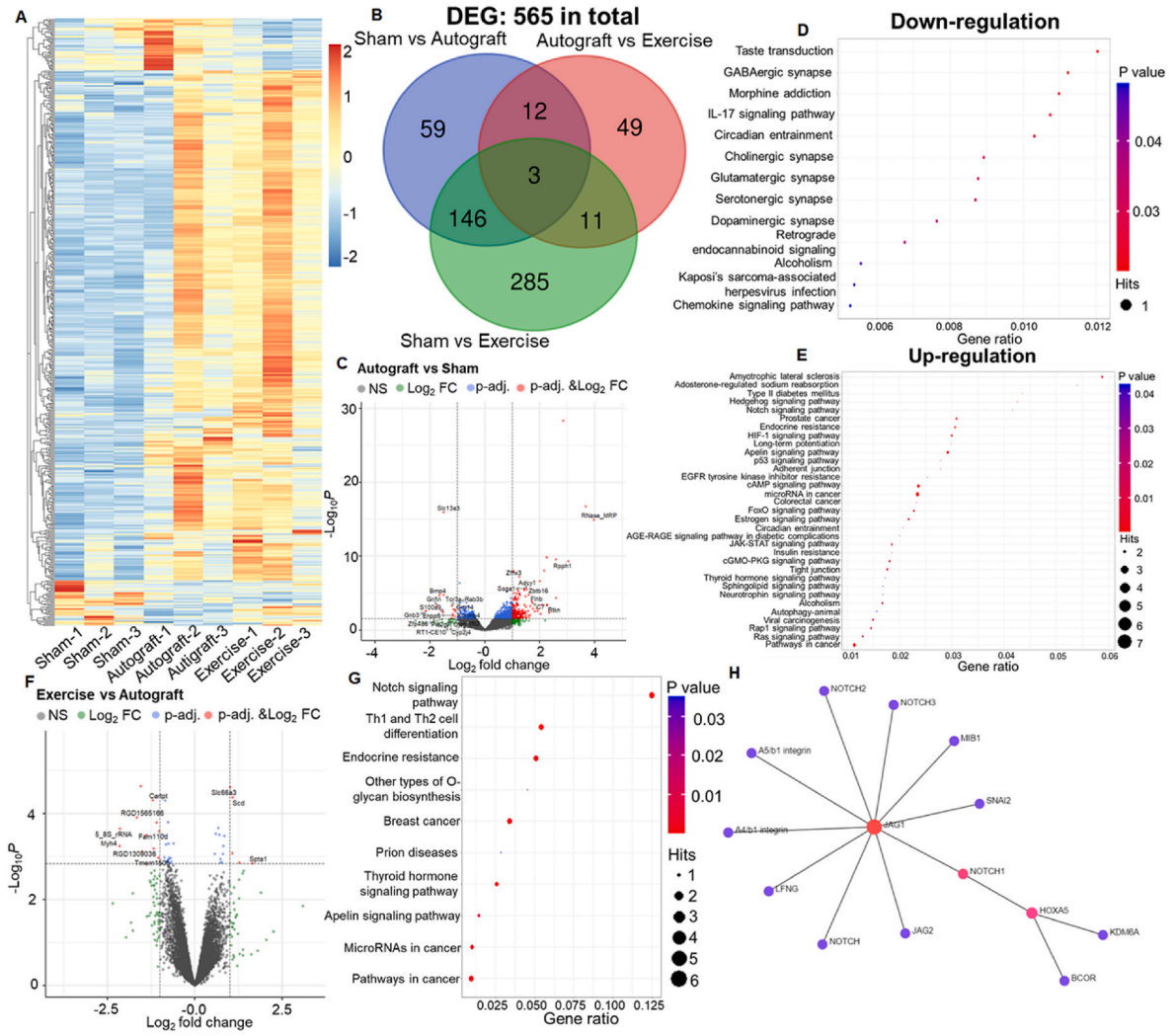

Fig. 6. Expression changes of total RNA at the ipsilateral SDH after a long-gap PNI and treadmill exercise by using RNA-Seq assay. a Heat map showing hierarchical clustering of DEGs compared among Sham, Autograft, and Exercise groups; **b** Venn diagram illustrating the number of overlapping DEGs among the three groups; **c** Volcano plot displaying up- and down-regulated RNAs by comparing the Autograft group to the Sham group; **d-e** KEGG enrichment analysis of up- and down-regulated RNAs by comparing the Autograft group to the Sham group; **f** Volcano plot displaying up- and down-regulated RNAs by comparing the Exercise group to the Autograft group; **g-h** KEGG enrichment analysis (**g**) and PPI network analysis (**h**) of 71 selected DEGs. In the PPI network plot, red nodes indicate seed genes, while purple nodes indicate genes that have known interactions. (For interpretation of the references to color in this figure legend, the reader is referred to the Web version of this article.)

3.6. Long-gap nerve transection induces chronic microstructural and metabolite changes in supraspinal regions of interest (ROIs), and exercise partially reverses the alterations

At 16 weeks post-injury, *in vivo* MRI and MRS were performed to investigate structural and metabolite changes in the brain. DTI is an advanced MRI technique that measures the degree and directionality of water diffusion, thus reflecting the microstructural organization in tissues of interest. Based on DTI signals in the cerebral cortex (CTX), hippocampus, thalamus, and hypothalamus, the apparent diffusion coefficient (ADC) and fractional anisotropy (FA) were calculated (Supplementary Fig. 4A). The ADC quantitatively reflects the overall dispersion magnitude of water. The long-gap nerve injury and autograft repair significantly decreased the ADC value in the right hippocampus, bilateral thalamus, and left hypothalamus (Fig. 7A). Exercise did not cause recovery of these changes and further decreased the ADC in the left CTX and right hypothalamus. The decreased ADC indicated a restriction of water motion, which may be associated with an increased cellularity, such as astrocytic and microglial activation. The FA is a measure of anisotropy of water diffusion along neural axon tracts, with a higher FA value reflecting highly anisotropic diffusion, and a lower FA value indicating more isotropic diffusion. The PNI resulted in a decrease of the FA value in the left hippocampus and bilateral thalamus, while exercise reversed the change in the hippocampus but not in the thalamus (Fig. 7B). The decreased FA represented a weakened water diffusion traveling along the direction of nerve fibers, which could be a result of the axonal loss, disrupted axonal membrane, and/or demyelination. All these results implicate that the nerve transection caused long-term microstructural changes in the hippocampus, thalamus, and hypothalamus, while the exercise had limited beneficial effects on the recovery of these changes.

Other than microstructural information, MRS can non-invasively measure concentrations of various metabolites *in vivo*. Thus, MR spectra was further acquired from the CTX, hippocampus, and thalamus to investigate the physiological changes after the long-gap nerve injury (Fig. 7C and Supplementary Fig. 4B). Concentrations of six metabolites were measured and analyzed: NAA, Ins, tCHO, GABA, Glu, and Gln. NAA is widely acknowledged as an indicator for neuronal health and integrity, and the PNI did not change the level of NAA in the selected brain regions. Ins plays an important role in osmoregulation and is believed to

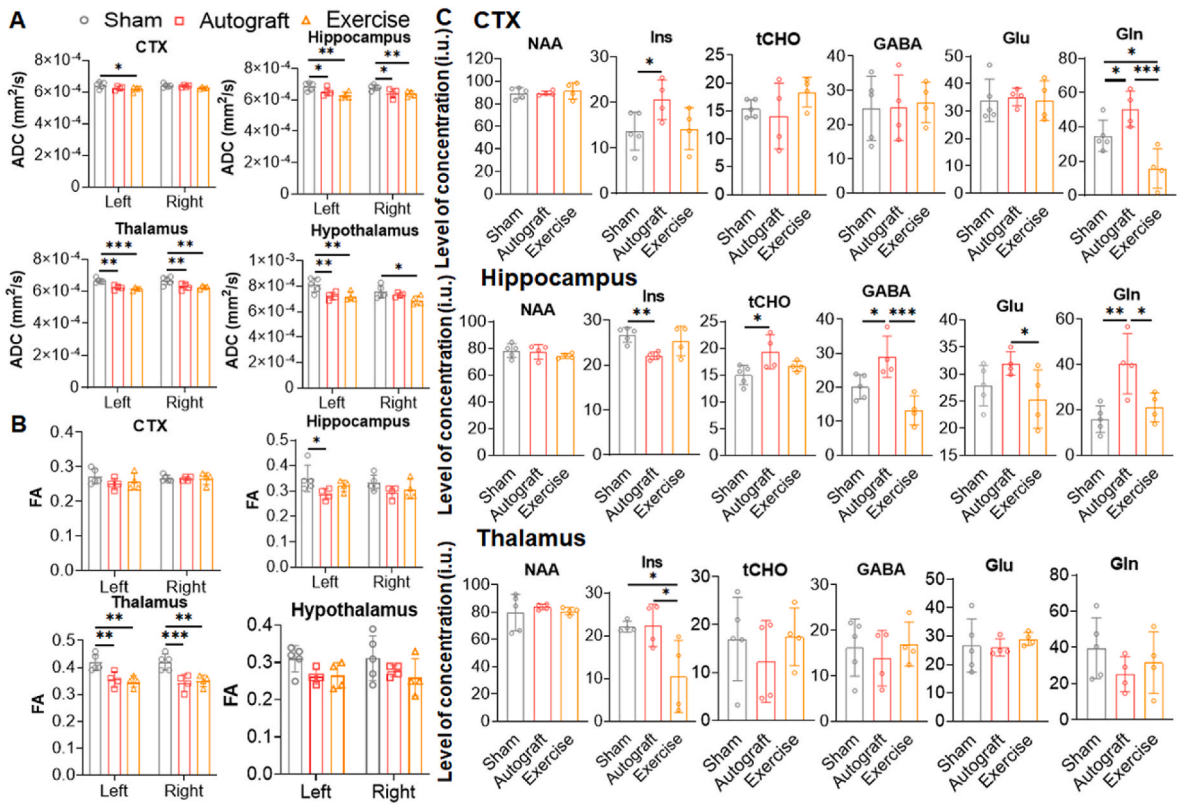

Fig. 7. Microstructural and metabolite changes in supraspinal ROIs after the long-gap PNI and treadmill exercise detected by DTI and MRS studies, respectively. A-B Differences in ADC (**A**) and FA (**B**) at the CTX, hippocampus, thalamus, and hypothalamus of right and left hemispheres; **C** Calibrated concentrations of NAA, Ins, tCHO, GABA, Glu, and Gln in the CTX, hippocampus, and thalamus. (n = 4 or 5, *p < 0.05, **p < 0.01, ***p < 0.001).

be primarily located in glial cells. The MRS results revealed an increase of Ins in the CTX and a decrease in the hippocampus in the Autograft group. The exercise after PNI reversed these changes, but, meanwhile, caused an additional decrease of Ins in the thalamus. Metabolite choline is used to reflect cell membrane biosynthesis and turnover. In the Autograft group, there was an increase of the tCho level in the hippocampus, which disappeared in the Exercise group. Moreover, Glu and GABA are the brain's major excitatory and inhibitory neurotransmitters, respectively, which could be taken up by astrocytes after the release from neurons and converted to Gln as a storage precursor. MRS results indicated that the long-gap PNI triggered an increase of both GABA and Glu in the hippocampus, while the exercise significantly reduced their levels. In addition, the levels of the Gln were increased in the CTX as well as in the hippocampus, which were decreased after the treadmill exercise. Altogether, results from the DTI and MRS demonstrated that traumatic PNI would cause persistent changes in the microstructural and metabolic processes in the supraspinal regions, and exercise could further partially regulate these changes.

3.7. Exercise partially reverses long-gap PNI-induced volumetric reorganization as well as maladaptive changes of neural activity in supraspinal regions

The long-term plastic changes and sustained activation in the brain were further examined by using MEMRI. Mn^{2+} can be transported into excitable cells in the nervous system through voltage-gated Ca^{2+} channels, thus enhancing signals with T1-weighted MRI (Massaad and Pautler, 2011). To investigate structural changes and neural activity in supraspinal areas involved in the pain processing, multiple ROIs were selected, including the primary somatosensory cortex of the hind limbs (S1HL), secondary somatosensory cortex (S2), motor cortex 1/2 (MC), cingulate cortex (CC), periaqueductal grey (PAG), insular cortex (IC), amygdala, thalamus, hypothalamus, hippocampus, prelimbic system (PrL), and basal forebrain (BF), which were schematically depicted in Fig. 8A. The T1 signal was visualized in Fig. 8B and further extracted from the ROIs for statistical analysis. Regarding structural changes of ROIs, rats from the Autograft group exhibited a volumetric increase in the amygdala and reduction in the CC, which were reversed by exercise (Fig. 8C). In addition, the PNI slightly decreased the volume of S1HL, while exercise significantly prevented this decrease in the left hemisphere of the brain (Supplementary Fig. 5A). Meanwhile, PNI also caused a size decease in the CC and thalamus in the right hemisphere of the brain. To further investigate differential impacts of the PNI and exercise on ROIs in the left and right brain hemispheres, relative volumetric changes in ROIs were further calculated (Supplementary Fig. 5B). The PNI caused a significant size reduction in the thalamus and MC on the right side as well as the PrL and hypothalamus on the left side compared to the other sides. These changes were ameliorated to some extent by treadmill running.

Furthermore, neural activities in ROIs have been determined based on the T1 signal intensity, with stronger signals indicating more neural activities. The signal intensity from the whole area of the ROIs was calculated (Fig. 8D). The T1 signal intensities in the S1HL, MC, CC, PrL, and S2 were significantly increased after the nerve injury. Meanwhile, the signal intensities in the hippocampus, PAG, and hypothalamus were reduced. These changes could be reversed through the treadmill exercise. In addition, the exercise increased the neural activity in the IC and BF as well as decreased the signal in the amygdala. No significant difference has been noted in the thalamus. Furthermore, we found no significant difference in the signal intensity between ROIs in the left and right hemispheres of the brain (Supplementary Fig. 6). Overall, these results demonstrated that a long-gap nerve injury would induce chronic and bilateral structural reorganizations as well as changes of neural activities in the ROIs, which may further affect pain and emotional

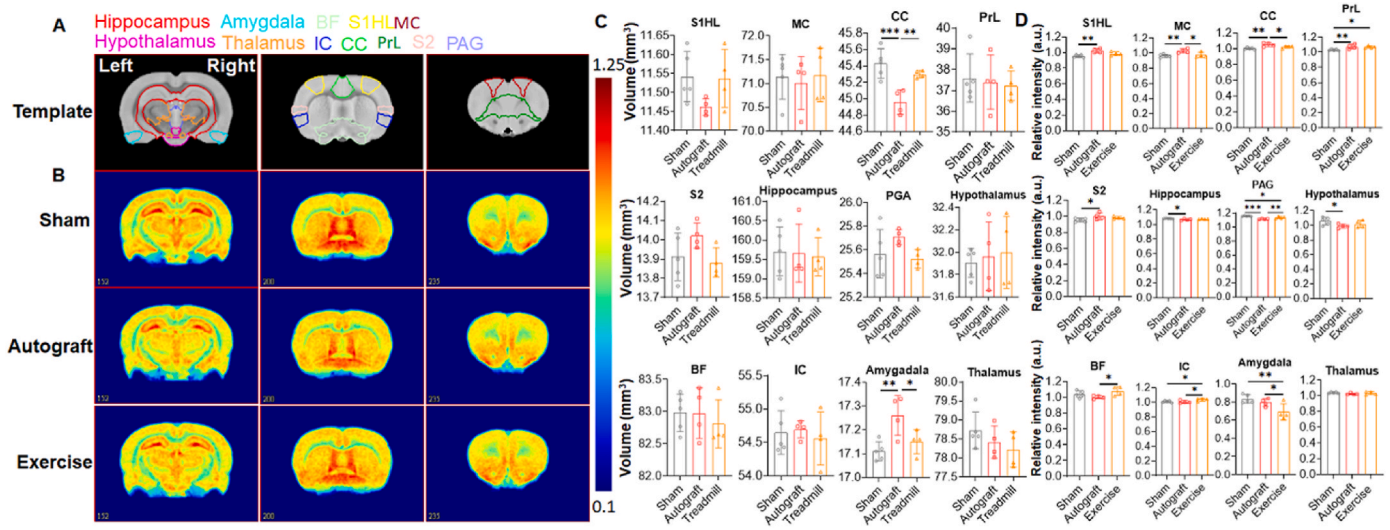

Fig. 8. Volumetric changes and neuronal activity in the brain after the long-gap PNI and treadmill exercise measured by T1-weighted MEMRI. a ROI analysis of the rat brain. ROIs were defined based on the SIGMA rat brain templates and atlases; **b** Color map of averaged T1-weighted images in each group. The color bar indicates normalized signal intensity; **c-d** Overall volume (**c**) and neuronal activity (**d**) of ROIs in the brain based on T1-weighted signals. (n = 4 or 5, *p < 0.05, **p < 0.01, ***p < 0.001). (For interpretation of the references to color in this figure legend, the reader is referred to the Web version of this article.)

processing, and exercise could reverse some of these changes.

4. Discussion

In this study, we systematically investigated the therapeutic functions of treadmill exercise with clinically practical regime (i.e., delayed initiation and low intensity) after a long-gap peripheral nerve transection and autograft repair in a rat model. The therapy outcomes demonstrated that the exercise could prevent muscle atrophy, promote nerve regeneration, and thus improve locomotor functions and sensory functions. Moreover, we found that the exercise therapy further partially reversed the neuroplastic changes in the DRGs, spinal cord, and the supraspinal regions, and many of these maladaptive changes due to severe peripheral nerve injury were involved in pain transduction, perception, and modulation.

It has been widely acknowledged that exercise can enhance muscle reinnervation and thus improve motor functions following PNIs (Gordon and English, 2016). Consistently, our study also found that low intensity exercise with late initiation increased the muscle mass and prevented myofiber atrophy. Chronic denervation following severe PNI, or with delayed repair, can further deleteriously impair the capability to restore muscle function even after reinnervation (Gordon et al., 2011; Sakuma et al., 2016). The abortive myogenesis and unsalvageable functional impairment during chronic denervation are partially due to the decline in number of muscular satellite cells. In response to nerve or muscle damage, satellite cells can become activated to proliferate and differentiate into myoblasts, which further fuse into myofibers and thus promote muscle regeneration. However, long-term denervation would exhaust the satellite cell pool and progressively reduce the satellite cell population in the skeletal muscles (Wong and Pomerantz, 2019; Carlson, 2014; Dedkov et al., 2001). We found that daily treadmill training increased the local density of satellite cells in the denervated gastrocnemius muscle. Previous studies also reported that exercise can contribute to muscle hypertrophy through activating satellite cells (Bazgir et al., 2017). Therefore, exercise can promote muscle recovery via mediating the activation of satellite cells, and, meanwhile, it probably also benefits in maintaining the capability of myogenesis during long-term recovery from PNIs. Several studies also evaluated the locomotor function recovery via exercise based on limb movements and kinematics, although the outcome was not consistent. It has been demonstrated that exercise enhanced locomotor function by increasing step height and length as well as improving hindlimb movement patterns (Zhang et al., 2014; Boeltz et al., 2013). However, one study reported that, despite increasing the muscular-evoked electromyographic intensity, exercise had no significant benefit in either hindlimb length or limb orientation during animal walking (Cannoy et al., 2016). In this study, the step movement was visualized by using a rat-walking system followed by kinematic analysis with MouseWalker software (Mendes et al., 2015; Kappos et al., 2017). We found that exercise can benefit the coordination during walking, with better controlled falling positions and improved stance/swing phases of the denervated hindlimb. Nevertheless, we also found that the rats from both injury groups failed to exert sufficient force to support their bodies with their injured hindlimbs during walking. This result could be consistent with previous studies that report that reinnervation at the soleus muscle following PNI was extremely poor and that treadmill exercise was ineffective for recovering soleus muscular functions (Cannoy et al., 2016; Ijkema-Paassen et al., 2002). Besides, it may also partially result from PNI-induced pain, as we observed a high expression of one of the typical pain-associated markers, TRPV1 receptor, at the ipsilateral lumbar DRG neurons. It has also been reported that, after long-gap nerve transection, rats also performed hypersensitive responses to mechanical stimuli during the recovery from sensory loss (Meyer et al., 2016a, 2016b). Suffering from the pain generated in injured hindlimbs, the animals may avoid using enough pressure on the limb to support their regular movement.

Nerve transection can also cause chronic sensory loss to both mechanical and thermal stimuli, while the effects of exercise on sensory function recovery are limitedly reported in previous studies. Several studies demonstrated that early exercise initiation following nerve transection promoted the restoration of sensations (Asensio-Pinilla et al., 2009; Cobianchi et al., 2013). In our study, the sensation in response to both mechanical and noxious heat stimuli had a gradual recovery over several weeks after the injury and repair, followed by a plateaued recovery. Later recovery was slow, while the exercise training further decreased the withdrawal latency in response to noxious heat to the heathy level. Although a stronger mechanical force was still required to elicit a paw withdrawal after the exercise training at the end of observation, this insensitive response to the stimulus is not necessarily related to a delayed or impaired recovery of sensory functions. As mentioned above, the withdrawal response is a composite reaction affected by both PNI-caused sensory deficits and pain (Osborne et al., 2018). Meanwhile, exercise has been reported to enhance pain tolerance

in healthy individuals by decreasing pain sensitivity, known as exercise-induced hypoalgesia (Vaegter et al., 2017; Jones et al., 2014). In addition, it has been well established that exercise interventions are beneficial for relieving neuropathic pain, which manifests as increased withdrawal thresholds in response to stimuli (Cobianchi et al., 2013; Dobson et al., 2014). Thus, both of these effects from the exercise can contribute to an increased tolerance to a mechanical stimulus.

Improvements observed in sensorimotor functions could be attributed to the faster nerve regeneration observed in the group with treadmill exercise. The potential of exercise to support nerve regeneration has been extensively reported (Maugeri et al., 2021). Here, we demonstrated that exercise with late initiation also promoted nerve fiber growth and remyelination. Particularly, regenerative axons were arrested at the autograft and formed neural coil structures, while treadmill training resulted in better axonal alignment. After any nerve injury, especially a severe nerve transection injury, unrepaired nerves will produce chaotic regrowth of axons with extreme misdirection, consequently forming a traumatic neuroma, which can not only cause inefficient reinnervation of target tissue but also induce pain sensitization (Alant et al., 2013; Pan et al., 2021). Exercise can reduce axonal misdirection during nerve regeneration, which is probably dependent on neurotrophic factors secreted from SCs and/or neurons themselves (Sabatier and English, 2015; English et al., 2011).

Moreover, we also found a high expression of TNF-α in the autografts, implying a strong inflammatory activity at even 16 weeks post-injury. Excessive and chronic local inflammation could be harmful to neural axons and also cause neuropathic pain (McDonald et al., 2007). Various types of inflammatory factors, such as TNF-α, can upregulate and sensitize TRPV1 receptors on primary sensory neurons, thus leading to inflammation- and/or PNI-induced pain (Moore et al., 2018; Malek et al., 2015). The overexpression of TRPV1 in the DRG sensory neurons implicated that the nerve transection not only caused loss of sensation but probably also induced pain. Although the mechanism is still elusive, numerous studies have reported that exercise can reduce the inflammation in chronic nerve injury and meanwhile relieve the pain (Chen et al., 2012; Kami et al., 2017; Safakhah et al., 2017; Sun et al., 2018). Consistently, current study demonstrated that the treadmill exercise with late initiation suppressed the chronic inflammation and prevented the upregulation of TRPV1 in the DRG after PNI, which might implicate a potential mechanism for the analgesic effects of exercise-based therapy.

PNI can also induce plastic changes in the CNS. Nevertheless, the impacts of exercise on the central plasticity after PNI have only been limitedly discussed. Firstly, in the spinal cord, a long-gap nerve transection induced a chronic and bilateral microglial activation, but we did not see differential expression of TNF-α at 16 weeks post-injury. This result is consistent with previous studies, demonstrating that an acute production of pro-inflammatory mediators, such as TNF-α, after PNI causes the development of pain, while the maintenance of pain in the chronic phase should be attributed to other mechanisms (e.g., neurotrophin signaling) (Echeverry et al., 2017; Taves et al., 2013).

Moreover, based on RNA-Seq and KEGG enrichment analysis, the PNI triggered changes in multiple signaling pathways that are intimately associated with neuropathic pain and central sensitization. Firstly, the downregulated genes are involved in diverse synaptic signaling pathways. It has been well studied that the impairment of GABAergic inhibitory pathways at the SDH after PNI can cause the loss of inhibitory tone and thus contributes to neuropathic pain (Moore et al., 2002). Meanwhile, upregulations of cholinergic signaling and dopaminergic signaling at SDHs can exert analgesic effects, therefore the impairments of these pathways may implicate weakened anti-nociceptive modulations in the long term after PNIs (Chen et al., 2017b; Dhanasobhon et al., 2021). Serotonergic transmission plays a critical role in descending brainstem-spinal cord nociceptive modulations (Heijmans et al., 2021). Pain modulation via serotonergic projection is complicated and could be either inhibitory or faciliatory to nociceptive processing, depending on the receptor subtype being activated. Downregulation of serotonergic signaling suggests plastic changes of descending pain modulations in the long term after PNI, while the effects of this change need to be further investigated. However, contradictory to the finding of downregulation of glutamatergic signaling in our study, the SDH was found to enhance glutamatergic excitatory transmission during the weeks after a nerve lesion in a previous study (Inquimbert et al., 2012). Our opposite result could stem from the later time point of observation after the nerve injury. Glutamate is one of the major neurotransmitters released from primary sensory neurons. It has been reported that a peripheral nerve transection induced a delayed and progressive neuronal death that manifested several months later (Tandrup et al., 2000). Therefore, severe loss of sensory neurons as well as their central projections of primary afferent fibers during the late phase of nerve transection may result in the decreased glutamatergic transmission.

Secondly, several pathways of enrichment with upregulation after the PNI also intimately participate in pain generation. Activation of neurotrophin signaling at the peripheral nerves supports neuronal survival, axonal elongation, and myelination, whereas microglia-derived neurotrophic factors at the SDH can mediate the plastic changes of excitatory synaptic transmission, leading to central sensitization in the spinal cord (Richner et al., 2014). The activation of the JAK/STAT pathway in microglia has also been reported to induce the production of interleukin 6 in the spinal cord and thus contributes to neuropathic pain after nerve injury (Dominguez et al., 2008). Notch signaling has critical functions in determining cell fate in nervous system and may contribute to chronic pain (Sun et al., 2012). It has been reported that the activation of Notch signaling in the spinal cord can promote precursor cell development into excitatory neurons (Mizuguchi et al., 2006), astrocytes (Khazaei et al., 2020) and microglial cells (Grandbarbe et al., 2007). Meanwhile, Notch signaling is closely related to the activation of microglia inflammation and neurotoxic astrocytes after spinal cord injury (Jian et al., 2020; Qian et al., 2019), which could further result in central sensitization and chronic pain. Intrathecal administration of Notch inhibitors, such as DAPT, can prevent pain development as well as ameliorate pain following a PNI (Sun et al., 2012; Xie et al., 2015). In addition, Notch signaling has also been suggested to inhibit axon regeneration by disturbing the stabilization of microtubules and growth cone formation (Ferrari-Toninelli et al., 2008; Shi et al., 2011). Therefore, the deactivation of Notch signaling in the SDH may reflect that treadmill exercise could facilitate axon regeneration and, at the same time, relieve the PNI-induced chronic pain by regulating excitatory and inhibitory synaptic balance and glial activation in spinal cord.

Moreover, the *Hox* gene family is well-known for their important roles in embryonic and fetal development of the central nervous system (Lizen et al., 2017). It has also been reported that they participate in the assembly of neuronal circuitry, such as axonal growth and synaptogenesis (Gofflot and Lizen, 2018). However, their functions in PNIs and neuropathic pain have been rarely investigated. Our study demonstrated that HOX proteins may also participate in the central plasticity following a PNI and during the recovery process.

Emotional disorders, such as anxiety and depression, as well as learning, memory, and cognitive impairments are common comorbidities of PNIs, which are putatively considered to be closely related to maladaptive alterations in the brain during the PNI-induced pain (Fonseca-Rodrigues et al., 2021; Bushnell et al., 2013). Although exercise has been shown to improve cognitive and memory performances in an extensive range of diseases, its functions in the traumatic PNI and neuropathic pain have been limitedly discussed and reported. In the supraspinal regions, we found microstructural and volumetric reorganizations in the hippocampus, thalamus, hypothalamus, amygdala, and several areas of the CTX, such as the S1HL and CC, in the long term after a long-gap nerve transection. Some of them were reversed through exercise to some extent. Particularly, we also found metabolite changes and reduced neuronal activity in the hippocampus. The hippocampus is a key region for the processing of learning and memory. Clinical data

showed that a greater level of Gln and a lower level of Ins (Shawcross et al., 2004). Moreover, the enhancement of GABAergic transmission has been observed in rodents under stress and/or with intellectual disabilities (Hu et al., 2010; Fernandez and Garner, 2007). The hippocampus had similar changes after the nerve transection in our study, implicating that PNI-caused cognitive impairments, memory deficits, and deleterious stress could be partially due to metabolite changes in the hippocampus. In addition, by modulating metabolites in the hippocampus, exercise may be able to help alleviate PNI-associated neuropsychiatric syndromes.

Our findings in neuronal activation changes parallel previous studies that indicated an increased activation in the somatosensory cortex, MC, CC, and PrL cortex as well as a deactivation in the PAG in the late phase of PNI (Hubbard et al., 2015). Among them, the somatosensory cortex is responsible for processing somatic sensation throughout the body and is important for the localization and discrimination of pain, while the MC is crucial for initiating and controlling motor movements. The sustained activation of the somatosensory cortex and MC could be an attempt to compensate for the sensory and motor loss after the PNI. Moreover, hyperexcitability in the S1 has been suggested to contribute to chronic pain following the PNI (Kim et al., 2017). Pharmacological inhibition of the S1 neuron activation can attenuate pain (Eto et al., 2011). Therefore, reduced neuronal activities at the somatosensory cortex may reflect an analgesic effect of exercise on the PNI-induced pain. The CC is a critical region in emotional and motivational aspects of pain perception, and the inhibition of plastic changes in the frontal part of the CC can alleviate painful and anxious behaviors following the PNI (Li et al., 2010; Koga et al., 2015). The PrL division of the medial prefrontal cortex is also associated with cognitive and emotional functions, while PNI-induced chronic pain would cause morphological and functional plasticity in the PrL (Medeiros et al., 2020). Thus, the inhibition of plasticity at these areas through the treadmill exercise suggests that physical activity may help regulate emotion and improve cognitive functions after the PNI. Moreover, it has been reported that neuronal activation in the PrL cortex can induce defensive behaviors and innate fear-induced antinociception (de Freitas et al., 2014). MC stimulation is an effective strategy for treating chronic neuropathic pain by activating the PAG-mediated descending inhibitory pathway (Silva et al., 2015; Negrini-Ferrari et al., 2021). Maladaptive neuronal activation observed in these regions implies that animals attempted to induce defensive mechanisms to ameliorate associated pain after the long-gap nerve lesion. However, evidence also suggests that PNI can cause a GABAergic inhibition of projections from the PrL cortex to the PAG, which leads to hypoglutamatergic neurotransmission in the PAG (Ho et al., 2013; Huang et al., 2019). The increased inhibition in the PAG region would impair descending pain inhibition by reducing the noradrenergic and serotoninergic transmission at the SDH, which is aligned with our results from the RNA-Seq analysis. Herein, consistent with these studies, we also observed a deactivation in the PAG after the PNI. In addition, the hypothalamus is also a part of a descending system, and stimulation of the hypothalamus has been reported to increase the serotonin input at the SDH to produce antinociception (Holden et al., 2005). The deactivation in the hypothalamus after the PNI further suggests the dysfunction of descending modulation pathways. We infer that the activation of the PrL and MC failed to prevent the PAG inhibition after the PNI, and the compromised descending pain inhibition was not effective at alleviating the pain. Exercise may reduce the pain and relieve the stress so that the activation of the descending pain inhibition was not necessarily required, and plastic neuronal activation in the PrL, MC, and PAG was reversed.

Although our preliminary findings in brain reorganization suggest positive and promising effects of exercise intervention on PNI-related mental and cognitive disorders, a larger sample size is required to validate these relations. Another limitation is that here we merely tested the sensorimotor functions and, therefore, relevant behavioral tests for mental and psychological health as well as cognitive functions are still required to determine the benefits of exercise after PNI. In addition, how PNI and treadmill exercise-based therapy affect the neuroplasticity in the spinal cord and supraspinal regions need further in-depth investigation and validation at the cellular and molecular levels. Furthermore, the effects of exercise could be dependent on different parameters/regimes and the time window. The time of exercise onset and intensity is critical, which should be taken into consideration and be optimized. Meanwhile, the effect of exercise on PNI recovery is sex-dependent (Wood et al., 2012), implicating that there are sex differences in the effects of exercise intervention on the neural plasticity after long-gap nerve transection.

5. Conclusion

Collectively, our data demonstrated that low intensity treadmill exercise with late initiation facilitated the recovery of sensorimotor function, prevented muscle atrophy, and promoted nerve regeneration after a long-gap nerve transection with an autograft repair. These findings support the promising potential of exercise rehabilitation, as a non-pharmacological strategy, for clinical treatment of severe traumatic nerve injury. In addition, this study found that exercise partially reversed some plastic changes in both peripheral and central nervous systems after the PNI, implicating possible underlying mechanisms for the analgesic effect of exercise-based therapy. Relevant changes in the SDH and supraspinal regions, as discussed above, need to be further investigated, which may further provide therapeutic directions for modulating PNI-induced chronic pain.

Author contribution

Conceptualization: Y.F.K., B.D.; Methodology: Y.F.K., M.K., Y.S., Y.T.L, C.Z. Investigation: Y.F.K., M.K., Y.S., F.F., W.X., W.S., Y.T.L, B.D.; Funding acquisition: B.D.; Project administration: B.D.; Supervision: Y.T.L, C.Z, B.D.; Writing—original draft: Y.F.K., Y.S.; Writing—review & editing: M.K., Y.T.L, C.Z., Z.P., B.D.

Declaration of competing interest

The authors declare that there are no competing interests.

Data availability

Data will be made available on request.

Acknowledgement

This work has been supported by Mary & Dick Holland Regenerative Medicine Program pilot project grant, University of Nebraska Collaboration Initiative Grant and NIH (R21AR078439) (B.D.). The University of Nebraska Medical Center Bioimaging Core Facility is administrated through the Office of the Vice Chancellor for Research and supported by state funds from the Nebraska Research Initiative (NRI), NIH P30GM127200, P20GM130447, and P30MH062261 (CHAIN).

Appendix A. Supplementary data

Supplementary data to this article can be found online at https://doi.org/10.1016/j.bbih.2022.100556.

References

Alant, JDdV., Senjaya, F., Ivanovic, A., et al., 2013. The impact of motor axon misdirection and attrition on behavioral deficit following experimental nerve injuries. PLoS One 8 (11), e82546.

Almeida, C., DeMaman, A., Kusuda, R., et al., 2015. Exercise therapy normalizes BDNF upregulation and glial hyperactivity in a mouse model of neuropathic pain. Pain 156 (3), 504–513.

Anders, S., Pyl, P.T., Huber, W., 2015. HTSeq—a Python framework to work with high-throughput sequencing data. Bioinformatics 31 (2), 166–169.
Asensio-Pinilla, E., Udina, E., Jaramillo, J., et al., 2009. Electrical stimulation combined with exercise increase axonal regeneration after peripheral nerve injury. Exp. Neurol. 219 (1), 258–265.
Bade, A.N., Gendelman, H.E., Boska, M.D., et al., 2017. MEMRI is a biomarker defining nicotine-specific neuronal responses in subregions of the rodent brain. Am. J. Tourism Res. 9 (2), 601.
Bazgir, B., Fathi, R., Valojerdi, M.R., et al., 2017. Satellite cells contribution to exercise mediated muscle hypertrophy and repair. Cell J. (Yakhteh) 18 (4), 473.
Bobinski, F., Martins, D., Bratti, T., et al., 2011. Neuroprotective and neuroregenerative effects of low-intensity aerobic exercise on sciatic nerve crush injury in mice. Neuroscience 194, 337–348.
Bobinski, F., Ferreira, T.A.A., Córdova, M.M., et al., 2015. Role of brainstem serotonin in analgesia produced by low-intensity exercise on neuropathic pain following sciatic nerve injury in mice. Pain 156 (12), 2595.
Boeltz, T., Ireland, M., Mathis, K., et al., 2013. Effects of treadmill training on functional recovery following peripheral nerve injury in rats. J. Neurophysiol. 109 (11), 2645–2657.
Bolger, A.M., Lohse, M., Usadel, B., 2014. Trimmomatic: a flexible trimmer for Illumina sequence data. Bioinformatics 30 (15), 2114–2120.
Boska, M.D., Dash, P.K., Knibbe, J., et al., 2014. Associations between brain microstructures, metabolites, and cognitive deficits during chronic HIV-1 infection of humanized mice. Mol. Neurodegener. 9 (1), 1–18.
Bushnell, M.C., Čeko, M., Low, L.A., 2013. Cognitive and emotional control of pain and its disruption in chronic pain. Nat. Rev. Neurosci. 14 (7), 502–511.
Cannoy, J., Crowley, S., Jarratt, A., et al., 2016. Upslope treadmill exercise enhances motor axon regeneration but not functional recovery following peripheral nerve injury. J. Neurophysiol. 116 (3), 1408–1417.
Carlson, B.M., 2014. The biology of long-term denervated skeletal muscle. Eur. J. Transl. Myol. 24 (1).
Chen, Y.-W., Li, Y.-T., Chen, Y.C., et al., 2012. Exercise training attenuates neuropathic pain and cytokine expression after chronic constriction injury of rat sciatic nerve. Anesth. Analg. 114 (6), 1330–1337.
Chen, S.-P., Zhou, Y.-Q., Liu, D.-Q., et al., 2017a. PI3K/Akt pathway: a potential therapeutic target for chronic pain. Curr. Pharmaceut. Des. 23 (12), 1860–1868.
Chen, M., Hoshino, H., Saito, S., et al., 2017b. Spinal dopaminergic involvement in the antihyperalgesic effect of antidepressants in a rat model of neuropathic pain. Neurosci. Lett. 649, 116–123.
Cobianchi, S., Casals-Diaz, L., Jaramillo, J., et al., 2013. Differential effects of activity dependent treatments on axonal regeneration and neuropathic pain after peripheral nerve injury. Exp. Neurol. 240, 157–167.
Daly, W., Yao, L., Zeugolis, D., et al., 2012. A biomaterials approach to peripheral nerve regeneration: bridging the peripheral nerve gap and enhancing functional recovery. J. R. Soc. Interface 9 (67), 202–221.
de Freitas, R.L., Salgado-Rohner, C.J., Biagioni, A.F., et al., 2014. NMDA and AMPA/kainate glutamatergic receptors in the prelimbic medial prefrontal cortex modulate the elaborated defensive behavior and innate fear-induced antinociception elicited by GABAA receptor blockade in the medial hypothalamus. Cerebr. Cortex 24 (6), 1518–1528.
Dedkov, E.I., Kostrominova, T.Y., Borisov, A.B., et al., 2001. Reparative myogenesis in long-term denervated skeletal muscles of adult rats results in a reduction of the satellite cell population. Anat. Rec.: Off. Publ. Am. Assoc. Anat. 263 (2), 139–154.
Devonshire, I.M., Burston, J., Xu, L., et al., 2017. Manganese-enhanced magnetic resonance imaging depicts brain activity in models of acute and chronic pain: a new window to study experimental spontaneous pain? Neuroimage 157, 500–510.
Dhanasobhon, D., Medrano, M.-C., Becker, L.J., et al., 2021. Enhanced analgesic cholinergic tone in the spinal cord in a mouse model of neuropathic pain. Neurobiol. Dis. 155, 105363.
Ding, Z., Dai, C., Zhong, L., et al., 2021. Neuregulin-1 converts reactive astrocytes toward oligodendrocyte lineage cells via upregulating the PI3K-AKT-mTOR pathway to repair spinal cord injury. Biomed. Pharmacother. 134, 111168.
Dobson, J.L., McMillan, J., Li, L., 2014. Benefits of exercise intervention in reducing neuropathic pain. Front. Cell. Neurosci. 8, 102.
Dominguez, E., Rivat, C., Pommier, B., et al., 2008. JAK/STAT3 pathway is activated in spinal cord microglia after peripheral nerve injury and contributes to neuropathic pain development in rat. J. Neurochem. 107 (1), 50–60.
Echeverry, S., Shi, X.Q., Yang, M., et al., 2017. Spinal microglia are required for long-term maintenance of neuropathic pain. Pain 158 (9), 1792–1801.
English, A.W., Cucoranu, D., Mulligan, A., et al., 2009. Treadmill training enhances axon regeneration in injured mouse peripheral nerves without increased loss of topographic specificity. J. Comp. Neurol. 517 (2), 245–255.
English, A.W., Wilhelm, J.C., Sabatier, M.J., 2011. Enhancing recovery from peripheral nerve injury using treadmill training. Ann. Anat. Anat. Anzeiger 193 (4), 354–361.
Eto, K., Wake, H., Watanabe, M., et al., 2011. Inter-regional contribution of enhanced activity of the primary somatosensory cortex to the anterior cingulate cortex accelerates chronic pain behavior. J. Neurosci. 31 (21), 7631–7636.
Faroni, A., Mobasseri, S.A., Kingham, P.J., et al., 2015. Peripheral nerve regeneration: experimental strategies and future perspectives. Adv. Drug Deliv. Rev. 82, 160–167.
Fernandez, F., Garner, C.C., 2007. Over-inhibition: a model for developmental intellectual disability. Trends Neurosci. 30 (10), 497–503.
Ferrari-Toninelli, G., Bonini, S., Bettinsoli, P., et al., 2008. Microtubule stabilizing effect of notch activation in primary cortical neurons. Neuroscience 154 (3), 946–952.
Fonseca-Rodrigues, D., Amorim, D., Almeida, A., et al., 2021. Emotional and cognitive impairments in the peripheral nerve chronic constriction injury model (CCI) of neuropathic pain: a systematic review. Behav. Brain Res. 399, 113008.
Gofflot, F., Lizen, B., 2018. Emerging roles for HOX proteins in synaptogenesis. Int. J. Dev. Biol. 62 (11–12), 807–818.
Gordon, T., English, A.W., 2016. Strategies to promote peripheral nerve regeneration: electrical stimulation and/or exercise. Eur. J. Neurosci. 43 (3), 336–350.
Gordon, T., Tyreman, N., Raji, M.A., 2011. The basis for diminished functional recovery after delayed peripheral nerve repair. J. Neurosci. 31 (14), 5325–5334.
Grandbarbe, L., Michelucci, A., Heurtaux, T., et al., 2007. Notch signaling modulates the activation of microglial cells. Glia 55 (15), 1519–1530.
Heijmans, L., Mons, M.R., Joosten, E.A., 2021. A systematic review on descending serotonergic projections and modulation of spinal nociception in chronic neuropathic pain and after spinal cord stimulation. Mol. Pain 17, 17448069211043965.
Ho, Y.-C., Cheng, J.-K., Chiou, L.-C., 2013. Hypofunction of glutamatergic neurotransmission in the periaqueductal gray contributes to nerve-injury-induced neuropathic pain. J. Neurosci. 33 (18), 7825–7836.
Höke, A., 2006. Mechanisms of Disease: what factors limit the success of peripheral nerve regeneration in humans? Nat. Clin. Pract. Neurol. 2 (8), 448–454.
Holden, J., Farah, E.N., Jeong, Y., 2005. Stimulation of the lateral hypothalamus produces antinociception mediated by 5-HT1A, 5-HT1B and 5-HT3 receptors in the rat spinal cord dorsal horn. Neuroscience 135 (4), 1255–1268.
Hu, W., Zhang, M., Czéh, B., et al., 2010. Stress impairs GABAergic network function in the hippocampus by activating nongenomic glucocorticoid receptors and affecting the integrity of the parvalbumin-expressing neuronal network. Neuropsychopharmacology 35 (8), 1693–1707.
Huang, J., Gadotti, V.M., Chen, L., et al., 2019. A neuronal circuit for activating descending modulation of neuropathic pain. Nat. Neurosci. 22 (10), 1659–1668.
Hubbard, C.S., Khan, S.A., Xu, S., et al., 2015. Behavioral, metabolic and functional brain changes in a rat model of chronic neuropathic pain: a longitudinal MRI study. Neuroimage 107, 333–344.
Ijkema-Paassen, J., Meek, M.F., Gramsbergen, A., 2002. Reinnervation of muscles after transection of the sciatic nerve in adult rats. Muscle Nerve 25 (6), 891–897.
Inquimbert, P., Bartels, K., Babaniyi, O.B., et al., 2012. Peripheral nerve injury produces a sustained shift in the balance between glutamate release and uptake in the dorsal horn of the spinal cord. Pain 153 (12), 2422–2431.
Jian, Y., Dong, S., Xu, S., et al., 2020. MicroRNA-34a suppresses neuronal apoptosis and alleviates microglia inflammation by negatively targeting the Notch pathway in spinal cord injury. Eur. Rev. Med. Pharmacol. Sci. 24 (3), 1420–1427.
Jones, M.D., Booth, J., Taylor, J.L., et al., 2014. Aerobic training increases pain tolerance in healthy individuals. Med. Sci. Sports Exerc. 46 (8), 1640–1647.
Kami, K., Tajima, F., Senba, E., 2017. Exercise-induced hypoalgesia: potential mechanisms in animal models of neuropathic pain. Anat. Sci. Int. 92 (1), 79–90.
Kami, K., Tajima, F., Senba, E., 2020. Plastic changes in amygdala subregions by voluntary running contribute to exercise-induced hypoalgesia in neuropathic pain model mice. Mol. Pain 16, 1744806920971377.
Kappos, E.A., Sieber, P.K., Engels, P.E., et al., 2017. Validity and reliability of the CatWalk system as a static and dynamic gait analysis tool for the assessment of functional nerve recovery in small animal models. Brain Behav. 7 (7), e00723.
Khazaei, M., Ahuja, C.S., Nakashima, H., et al., 2020. GDNF rescues the fate of neural progenitor grafts by attenuating Notch signals in the injured spinal cord in rodents. Sci. Transl. Med. 12 (525), eaau3538.
Kim, Y.-J., Byun, J.-H., Choi, I.-S., 2015. Effect of exercise on μ-opioid receptor expression in the rostral ventromedial medulla in neuropathic pain rat model. Ann. Rehab. Med. 39 (3), 331.
Kim, W., Kim, S.K., Nabekura, J., 2017. Functional and structural plasticity in the primary somatosensory cortex associated with chronic pain. J. Neurochem. 141 (4), 499–506.
Kim, D., Paggi, J.M., Park, C., et al., 2019. Graph-based genome alignment and genotyping with HISAT2 and HISAT-genotype. Nat. Biotechnol. 37 (8), 907–915.
Koga, K., Descalzi, G., Chen, T., et al., 2015. Coexistence of two forms of LTP in ACC provides a synaptic mechanism for the interactions between anxiety and chronic pain. Neuron 85 (2), 377–389.
Kong, Y., Shi, W., Zhang, D., et al., 2021. Injectable, antioxidative, and neurotrophic factor-deliverable hydrogel for peripheral nerve regeneration and neuropathic pain relief. Appl. Mater. Today 24, 101090.
Li, X.-Y., Ko, H.-G., Chen, T., et al., 2010. Alleviating neuropathic pain hypersensitivity by inhibiting PKMζ in the anterior cingulate cortex. Science 330 (6009), 1400–1404.
Liao, C.-F., Yang, T.-Y., Chen, Y.-H., et al., 2017. Effects of swimming exercise on nerve regeneration in a rat sciatic nerve transection model. Biomedicine 7 (1).
Licata, L., Lo Surdo, P., Iannuccelli, M., et al., 2020. SIGNOR 2.0, the SIGnaling network open resource 2.0: 2019 update. Nucleic Acids Res. 48 (D1), D504–D510.
Lin, X., Wang, M., Zhang, J., et al., 2014. p38 MAPK: a potential target of chronic pain. Curr. Med. Chem. 21 (38), 4405–4418.
Lizen, B., Hutlet, B., Bissen, D., et al., 2017. HOXA5 localization in postnatal and adult mouse brain is suggestive of regulatory roles in postmitotic neurons. J. Comp. Neurol. 525 (5), 1155–1175.
Lizeth Castillo-Galvan, M., Maximiliano Martinez-Ruiz, F., de la Garza-Castro, O., et al., 2014. Study of peripheral nerve injury in patients attended by traumatism. Gac. Med. Mex. 150 (6), 527–532.
Lopez-Alvarez, V.M., Puigdomenech, M., Navarro, X., et al., 2018. Monoaminergic descending pathways contribute to modulation of neuropathic pain by increasing-intensity treadmill exercise after peripheral nerve injury. Exp. Neurol. 299, 42–55.
Love, M.I., Huber, W., Anders, S., 2014. Moderated estimation of fold change and dispersion for RNA-seq data with DESeq2. Genome Biol. 15 (12), 550.
Malek, N., Pajak, A., Kolosowska, N., et al., 2015. The importance of TRPV1-sensitisation factors for the development of neuropathic pain. Mol. Cell. Neurosci. 65, 1–10.

Mang, C.S., Peters, S., 2021. Advancing motor rehabilitation for adults with chronic neurological conditions through increased involvement of kinesiologists: a perspective review. BMC Sports Sci. Med. Rehab. 13 (1), 1–11.
Massaad, C.A., Pautler, R.G., 2011. Manganese-enhanced Magnetic Resonance Imaging (MEMRI), Magnetic Resonance Neuroimaging. Springer, pp. 145–174.
Maugeri, G., D'Agata, V., Trovato, B., et al., 2021. The role of exercise on peripheral nerve regeneration: from animal model to clinical application. Heliyon, e08281.
McDonald, D.S., Cheng, C., Martinez, J.A., et al., 2007. Regenerative arrest of inflamed peripheral nerves: role of nitric oxide. Neuroreport 18 (16), 1635–1640.
Meacham, K., Shepherd, A., Mohapatra, D.P., et al., 2017. Neuropathic pain: central vs. peripheral mechanisms. Curr. Pain Headache Rep. 21 (6), 1–11.
Medeiros, P., de Freitas, R.L., Boccella, S., et al., 2020. Characterization of the sensory, affective, cognitive, biochemical, and neuronal alterations in a modified chronic constriction injury model of neuropathic pain in mice. J. Neurosci. Res. 98 (2), 338–352.
Mendes, C.S., Bartos, I., Márka, Z., et al., 2015. Quantification of gait parameters in freely walking rodents. BMC Biol. 13 (1), 1–11.
Meyer, C., Stenberg, L., Gonzalez-Perez, F., et al., 2016a. Chitosan-film enhanced chitosan nerve guides for long-distance regeneration of peripheral nerves. Biomaterials 76, 33–51.
Meyer, C., Wrobel, S., Raimondo, S., et al., 2016b. Peripheral nerve regeneration through hydrogel-enriched chitosan conduits containing engineered Schwann cells for drug delivery. Cell Transplant. 25 (1), 159–182.
Mizuguchi, R., Kriks, S., Cordes, R., et al., 2006. Ascl1 and Gsh1/2 control inhibitory and excitatory cell fate in spinal sensory interneurons. Nat. Neurosci. 9 (6), 770–778.
Moore, K.A., Kohno, T., Karchewski, L.A., et al., 2002. Partial peripheral nerve injury promotes a selective loss of GABAergic inhibition in the superficial dorsal horn of the spinal cord. J. Neurosci. 22 (15), 6724–6731.
Moore, C., Gupta, R., Jordt, S.-E., et al., 2018. Regulation of pain and itch by TRP channels. Neurosci. Bull. 34 (1), 120–142.
Negrini-Ferrari, S.E., Medeiros, P., Malvestio, R.B., et al., 2021. The primary motor cortex electrical and chemical stimulation attenuates the chronic neuropathic pain by activation of the periaqueductal grey matter: the role of NMDA receptors. Behav. Brain Res. 415, 113522.
Osborne, N.R., Anastakis, D.J., Davis, K.D., 2018. Peripheral nerve injuries, pain, and neuroplasticity. J. Hand Ther. 31 (2), 184–194.
Pan, D., Bichanich, M., Wood, I.S., et al., 2021. Long Acellular nerve allografts cap transected nerve to arrest axon regeneration and Alter upstream gene expression in a rat neuroma model. Plast. Reconstr. Surg. 148 (1), 32e–41e.
Park, J.-S., Höke, A., 2014. Treadmill exercise induced functional recovery after peripheral nerve repair is associated with increased levels of neurotrophic factors. PLoS One 9 (3), e90245.
Qian, D., Li, L., Rong, Y., et al., 2019. Blocking Notch signal pathway suppresses the activation of neurotoxic A1 astrocytes after spinal cord injury. Cell Cycle 18 (21), 3010–3029.
Richner, M., Ulrichsen, M., Elmegaard, S.L., et al., 2014. Peripheral nerve injury modulates neurotrophin signaling in the peripheral and central nervous system. Mol. Neurobiol. 50 (3), 945–970.
Sabatier, M.J., English, A.W., 2015. Pathways mediating activity-induced enhancement of recovery from peripheral nerve injury. Exerc. Sport Sci. Rev. 43 (3), 163.
Safakhah, H.A., Kor, N.M., Bazargani, A., et al., 2017. Forced exercise attenuates neuropathic pain in chronic constriction injury of male rat: an investigation of oxidative stress and inflammation. J. Pain Res. 10, 1457.
Sakuma, M., Gorski, G., Sheu, S.H., et al., 2016. Lack of motor recovery after prolonged denervation of the neuromuscular junction is not due to regenerative failure. Eur. J. Neurosci. 43 (3), 451–462.
Schwarz, A.J., Danckaert, A., Reese, T., et al., 2006. A stereotaxic MRI template set for the rat brain with tissue class distribution maps and co-registered anatomical atlas: application to pharmacological MRI. Neuroimage 32 (2), 538–550.
Seminowicz, D.A., Laferriere, A.L., Millecamps, M., et al., 2009. MRI structural brain changes associated with sensory and emotional function in a rat model of long-term neuropathic pain. Neuroimage 47 (3), 1007–1014.
Seta, H., Maki, D., Kazuno, A., et al., 2018. Voluntary exercise positively affects the recovery of long-nerve gap injury following tube-bridging with human skeletal muscle-derived stem cell transplantation. J. Clin. Med. 7 (4), 67.
Shawcross, D., Balata, S., Olde Damink, S., et al., 2004. Low myo-inositol and high glutamine levels in brain are associated with neuropsychological deterioration after induced hyperammonemia. Am. J. Physiol. Gastrointest. Liver Physiol. 287 (3), G503–G509.
Shi, M., Liu, Z., Lv, Y., et al., 2011. Forced notch signaling inhibits commissural axon outgrowth in the developing chick central nerve system. PLoS One 6 (1), e14570.
Siemionow, M., Brzezicki, G., 2009. Current techniques and concepts in peripheral nerve repair. Int. Rev. Neurobiol. 87, 141–172.
Silva, G.D., Lopes, P.S., Fonoff, E.T., et al., 2015. The spinal anti-inflammatory mechanism of motor cortex stimulation: cause of success and refractoriness in neuropathic pain? J. Neuroinflammation 12 (1), 1–11.
Skaper, S.D., 2018. Neurotrophic Factors: an Overview. Neurotrophic Factors, pp. 1–17.
Stagg, N.J., Mata, H.P., Ibrahim, M.M., et al., 2011. Regular exercise reverses sensory hypersensitivity in a rat neuropathic pain model: role of endogenous opioids. J. Am. Soc. Anesthesiol. 114 (4), 940–948.
Sun, Y.-Y., Li, L., Liu, X.-H., et al., 2012. The spinal notch signaling pathway plays a pivotal role in the development of neuropathic pain. Mol. Brain 5 (1), 1–6.
Sun, Y., Liu, J.Q., Tian, F., 2018. Exercise intervention alleviates nerve injury by the suppression of inflammatory mediator expression via the TLR4/NF-κB signaling pathway. Exp. Ther. Med. 16 (4), 2922–2930.
Tandrup, T., Woolf, C.J., Coggeshall, R.E., 2000. Delayed loss of small dorsal root ganglion cells after transection of the rat sciatic nerve. J. Comp. Neurol. 422 (2), 172–180.
Taves, S., Berta, T., Chen, G., et al., 2013. Microglia and spinal cord synaptic plasticity in persistent pain. Neural Plast. 2013.
Taylor, K.S., Anastakis, D.J., Davis, K.D., 2009. Cutting your nerve changes your brain. Brain 132 (11), 3122–3133.
Tkáč, I., Starčuk, Z., Choi, I.Y., et al., 1999. In vivo 1H NMR spectroscopy of rat brain at 1 ms echo time. Magn. Reson. Med.: Off. J. Int. Soc. Magn. Reson. Med. 41 (4), 649–656.
Uberti, M.G., Boska, M.D., Liu, Y., 2009. A semi-automatic image segmentation method for extraction of brain volume from in vivo mouse head magnetic resonance imaging using constraint level sets. J. Neurosci. Methods 179 (2), 338–344.
Vaegter, H., Hoeger Bement, M., Madsen, A., et al., 2017. Exercise increases pressure pain tolerance but not pressure and heat pain thresholds in healthy young men. Eur. J. Pain 21 (1), 73–81.
Wijnen, J.P., van Asten, J.J., Klomp, D.W., et al., 2010. Short echo time 1H MRSI of the human brain at 3T with adiabatic slice-selective refocusing pulses; reproducibility and variance in a dual center setting. J. Magn. Reson. Imag. 31 (1), 61–70.
Wilhelm, J.C., Xu, M., Cucoranu, D., et al., 2012. Cooperative roles of BDNF expression in neurons and Schwann cells are modulated by exercise to facilitate nerve regeneration. J. Neurosci. 32 (14), 5002–5009.
Wong, A., Pomerantz, J.H., 2019. The role of muscle stem cells in regeneration and recovery after denervation: a review. Plast. Reconstr. Surg. 143 (3), 779–788.
Wood, K., Wilhelm, J.C., Sabatier, M.J., et al., 2012. Sex differences in the effectiveness of treadmill training in enhancing axon regeneration in injured peripheral nerves. Dev. Neurobiol. 72 (5), 688–698.
Wu, S., Kuss, M., Qi, D., et al., 2019. Development of cryogel-based guidance conduit for peripheral nerve regeneration. ACS Appl. Bio Mater. 2 (11), 4864–4871.
Xie, K., Jia, Y., Hu, Y., et al., 2015. Activation of notch signaling mediates the induction and maintenance of mechanical allodynia in a rat model of neuropathic pain. Mol. Med. Rep. 12 (1), 639–644.
Yang, S., Chang, M.C., 2019. Chronic pain: structural and functional changes in brain structures and associated negative affective states. Int. J. Mol. Sci. 20 (13), 3130.
Zhang, L., Kaneko, S., Kikuchi, K., et al., 2014. Rewiring of regenerated axons by combining treadmill training with semaphorin3A inhibition. Mol. Brain 7 (1), 1–17.
Zhou, G., Soufan, O., Ewald, J., et al., 2019. NetworkAnalyst 3.0: a visual analytics platform for comprehensive gene expression profiling and meta-analysis. Nucleic Acids Res. 47 (W1), W234–W241.